Tyr181, the Van der waals interactions on 5,6-substituent position with surrounding amino acid residues (F227, V106, L234 and Y188) and the hydrophobic interactions of the R group on benzoxazin-2-one ring with the aromatic side chain of W229 and Y188 serve as significant interactions for the particular inhibition.

The docked conformations of efavirenz derivatives derived from GOLD and Autodock methods reveal very similar orientations in the WT and K103N RT binding pockets. However, based on lower rmsd of the docked pose from the X-ray pose of efavirenz, the docked conformations derived from Autodock method has been selected for further study on 3D-QSAR analysis and interaction energy estimation using quantum chemical calculations.

QSAR Analysis

The conformation with the lowest final docked energy was selected for the structural alignment in 3D-QSAR analyses. CoMFA and CoMSIA studies were applied to determine relationships between structural properties and HIV-1 inhibitions, based on the docked conformations.

CoMFA models

Two different types of biological activities were considered, WT and K103N HIV-1 RT inhibitory activities. The models obtained from the analyses include steric and electrostatic field contributions. The statistical parameters of CoMFA models of compounds are summarized in Table 3. Regarding WT HIV-1 RT inhibition, the best predictive ability QSAR model with r_{cv}^2 of 0.662, s-press = 0.145 and noc = 3, is obtained. The steric and electrostatic contributions of this model are 63.8 % and 36.2 %, respectively. Other statistical results of the best CoMFA model are the

conventional r^2 ($r^2 = 0.936$) and the standard error of estimation (0.066). F is 83.441 and the probability (P) of obtaining this value of F if r^2 is actually zero (probability of $r^2 = 0$) is lower than 0.001. The plot between predicted and experimental WT HIV-1 RT inhibitory affinities of the non-cross-validated analysis of the model is presented in Figure 7a.

For further analysis, the CoMFA results with respect to K103N HIV-1 RT inhibition were investigated. The high predictive model with r^2_{cv} of 0.755, s-press = 0.302 and noc = 6, is produced, shown in Table 3. The model has 51.2 % contribution from the steric field and 48.8 % contribution from electrostatic field, showing approximately equal contributions for explanation of the K103N inhibitory activities. The statistical parameters obtained are that the conventional r^2 is 0.944, the standard error of estimation is 0.144, F is equal to 107.318 and the probability (P) of obtaining this value of F if r^2 is actually zero (probability of r^2 = 0) is lower than 0.001. The plot between predicted and experimental K103N HIV-1 RT inhibitory affinities of the non-cross-validated analysis of the model is presented in Figure 7b.

Prediction for compounds in the test set

As the obtained CoMFA models, listed in Table 3, show reasonable predictive power for WT and K103N RT inhibition, both models were used to predict the inhibitory activities of 7 efavirenz derivatives in the test set. The comparison of predicted and observed biological activities of these compounds is listed in Table 5 and plotted in Figures 7a and 7b, respectively. Based on the residual value, the inspection of the data reveals the usefulness of the models for the prediction of the activities of the efavirenz compounds which are not included in the training set.

CoMSIA analysis

The results of CoMSIA studies were presented in Table 4. CoMSIA analysis was performed using five different property fields (steric, electrostatic, hydrophobic, hydrogen bond donor and hydrogen bond acceptor fields). In the present study, the propose of using five different descriptors is not to increase the significance and the predictive ability of the 3D QSAR models but to partition the various properties into the spatial location where they play a decisive role in determining biological activity. Comparing with the obtained CoMFA model, the best CoMSIA model corresponding to the WT HIV-1 RT inhibition reveals improved predictive ability than CoMFA model with a high predictive model (r^2_{cv} of 0.708, s-press = 0.142 and noc = 6). The other statistical results are that the conventional r^2 value is 0.894, the standard error of estimation is 0.085 and F is equal to 50.844. The corresponding field contributions of these five descriptor variables are 12.2, 19.5, 24.1, 16.8 and 27.3, respectively. The experimental and calculated affinities derived from the CoMSIA model for the WT inhibitory affinity is plotted in Figure 8a.

According to the K103N HIV-1 RT inhibition, the best CoMSIA model with the combination of all fields yielded high predictive ability with r^2_{cv} of 0.773, s-press = 0.286, noc = 3, the conventional r^2 = 0.938, the standard error of estimation = 0.155 and F = 93.344. The steric, electrostatic, hydrophobic, hydrogen bond donor and hydrogen bond acceptor field contributions of the model are 13.4, 22.3, 20.5, 26.5 and 17.3, respectively. The experimental and calculated affinities derived from the CoMSIA model for the K103N inhibitory affinity is plotted in Figure 8b.

Prediction for compounds in the test set

In order to evaluate the predictive ability of the resulting CoMSIA models, the same 7 efavirenz derivative tested set as used in CoMFA study was employed to predict the inhibitory activities. The comparison of predicted and observed biological activities of these compounds for WT and K103N inhibition, is reported in Table 6 and plotted in Figures 8a and 8b, respectively. The good correlation shows the validation of the obtained CoMSIA models for efavirenz derivatives excluded from the training set.

Graphical interpretation of Fields

CoMFA Contributions

The 3D–QSAR contour maps obtained from CoMFA results for all efavirenz derivatives illustrate clearly the steric and electrostatic contributions for ligand binding. To better understand the field interactions between the enzyme and inhibitors, the amino acid residues surrounding efavirenz compound in the binding pocket were merged into the contour mapsu. Sterically unfavorable regions are depicted in yellow, whereas favorable regions are in green. Electrostatic positive favorable regions correspond to the blue areas and the negative favorable regions correspond to the red areas.

The steric and electrostatic field contributions to WT HIV-1 RT inhibition is shown in Figure 9a. Compound 25, the most potent compound active against WT HIV-1 RT of the series, is used as a reference structure. There is a prominent blue

contour located between the C6 and C7 positions on the benzoxazin-2-one ring. It reveals that incorporation of electropositive group at this position would be preferable for the activity. This suggestion is supported by experimental data that, as clearly examples, compound 25 having hydrogen atom attached to the C6 position produces higher potency compared to compounds with halogen groups attached to the similar position (compounds 28, 30, 33, 34, 36, 38, 47, 50 and 53). Particularly, compound 25 shows the highest potency for the WT inhibition in the data set. There are large green contours corresponding to the location of the R substituent attached to the C4 position on the benzoxazin-2-one ring. However, the tolerated steric requirements of this region are highlighted by yellow contours presented around that region, especially a yellow one overlapping with the Tyr188 residue. It is indicated that an additional bulky group at this site would be favorable for the affinity, but the size and the dimension of the substituents should not be too large. This means that steric occupancy with too bulky groups of the sidechain leads to a steric conflict resulting in diminished favorable interactions with the aromatic ring of Y188. These suggestions agree well with the trend observed experimentally, reported in Table 1, that the cyclopropyl acetylene group is the optimum sidechain for this position. Compound 1 with the cyclopropyl acetylene group attached at the C4 substituent shows higher potency. Compounds 2-5 and 12-18, occupying the C4 site with too large substituents, result in significantly reduced potency against WT RT. A large blue electrostatic contour area close to the cyclopropyl group of the R position suggests that electropositive groups are predicted to increase activity in those areas. This suggestion agrees with the experimental data that compounds containing small heterocyclic rings having more electron rich properties, such as pyridyl, furanyl or thienyl groups (compounds 2-9), have diminished affinities against WT RT, compared to compound 1.

The contributions of steric and electrostatic fields to K103N RT inhibition is shown in Figure 9b. The most potent compound active against K103N HIV-1 RT of the series, compound 50, is put in the contour as a reference structure. Interestingly, the large blue contour located close to the C6 position on the phenyl ring is completely absent, compared to the WT inhibition. There are two red contours presented in the vicinity of the substituent attached to C6 position instead. A sterically favored green area is located in the region of the C5 substituent attached to the phenyl ring. It can be summarized that, in contrast to the WT inhibition, compounds having a bulky group attached to the C5 position and the preference of electronegative groups at the C6 position are more favorable for the K103N inhibition. This is in agreement with the experimental observation that compounds having sterically 5,6-halogen substituents (compounds 28, 33 and 36) confer higher potency against the K103N mutant compared to 5-halogen analogues (compounds 25 and 27). Compounds 50,51 and 53, occupying the C5 position with bulkier groups such as methoxy or hydroxyl group and the C6 position with chlorine atom, yield higher potency compared to compounds 38 and 45, respectively. In particular, compound 50 shows the highest activity against K103N HIV-1 RT in the data set. This could be the reason why compound 25, the highest active compound against WT HIV-1 RT, shows a significantly reduced potency against K103N RT. A blue contour close to Z substituent of the benzoxazin-2-one ring suggests that a group with low electron density would play a favorable role in activity. This suggestion is consistent with the experimental data that the replacement of an oxygen atom with the NH group at this

position always yields much more potent derivatives active against K103N RT, as exemplified by compounds 1, 2 compared to compounds 38 and 43, respectively. At the region close to the R position, a large green contour is still presented for the K103N RT inhibition and the yellow one overlapping with Y188 is also located close to approximately similar region. The structural requirements for this region could be explained in similar manner as those for WT RT inhibition. The structural requirements obtained from the CoMFA models for WT and K103N HIV-1 RT inhibition show high correspondence to molecular docking results previously described and QSAR studies reported [37,38].

CoMSIA Contributions

Additional to the steric and electrostatic fields used in CoMFA study, hydrophobic, hydrogen bond donor and hydrogen bond acceptor fields contributing to binding affinities can be derived from the CoMSIA models. To better understand the field interactions between the enzyme and inhibitors, the amino acid residues surrounding the efavirenz compound in the binding pocket were merged into the contour maps. In the present study, since the CoMSIA steric and electrostatic contours (not shown) are similarly placed as those of the CoMFA models, only hydrophobic, hydrogen bond donor and hydrogen bond acceptor field contributions were discussed further. The magenta and white regions highlight areas where hydrophilic and hydrophobic properties are preferable, respectively. The cyan contours indicate region where hydrogen bond donor groups increase activity, whereas purple contours indicate region where hydrogen bond donor groups decrease activity. Hydrogen bond

acceptors are favored in areas indicated by orange contours, whereas white contours are areas where hydrogen bond acceptors are disfavored.

The contribution of hydrophobic fields to the WT inhibition is shown in Figure 10a. A predominant feature of the hydrophobic contour plot is the presence of a large pink contour corresponding to the locations of the groups attached to C5 and C6 positions. It reflects that introducing hydrophobic substituents at the positions would enhance the biological activity. As demonstrated, halogen groups attached to C5 or C6 positions on the benzoxazin-2-one ring (compounds 25-33, 36 and 38) yield increasing binding affinities. On the other hand, methoxy or hydroxyl groups attached to C5 or C6 positions (compounds 34, 39-40, 49-53) would not be preferable for binding affinities. Moreover, the favorable hydrophobic region is located close to the vicinity of the R substituent, attached to the C4 position. As examples, more hydrophilic derivatives with alkoxy groups substituted at C4 (compounds 12-18) are less active for WT inhibition compared with compound 1. In contrast to WT inhibition, the contour map of hydrophobic properties highlights different areas for the K103N inhibition, as shown in Figure 10b. A white contour is presented near the substituent attached to C5 position. With the combination of the steric contour map obtained from CoMFA models, it suggests that the favorable hydrophilic together with steric substituents at the position could enhance the K103N RT inhibitory activity. This indicates that the bulky group with low hydrophobicity would be favorable to the biological activity, as demonstrated by compound 50, the highest active compound against K103N HIV-1 RT. A pink contour in the vicinity of the R4 substituent shows the importance of the hydrophobic component with an optimum steric bulk of the sidechain at the R4 position. This suggestion agrees well with the

experimental report that the optimum sidechain for this position is the acetylene cyclopropyl group.

Figures 11a and 11b show the contributions of the hydrogen donor fields for the WT and K103N inhibition, respectively. For WT inhibition, two cyan contours located at the NH group of the benzoxazin-2-one ring and presented in the vicinity of Z substituent represents that placement of hydrogen-bond donors at the positions is beneficial for the receptor binding. This could be attributed to the hydrogen bond interaction between the main chain carbonyl oxygen of K101 and the amide NH of efavirenz compound [25]. For the K103N inhibition shown in Figure 11b, the cyan contour located at the NH group of the benzoxazin-2-one ring is completely absent, while a cyan contour close to the Z substituent is presented. The minor cyan contour corresponds to the hydrogen donor substituent preferable at this position. This could be the reason that compounds having NH group as the Z substituent are more preferable for the K103N inhibitory activity than that of O atom. The contribution is consistent with the docking study and the electrostatic contribution derived from the CoMFA model.

The hydrogen bond acceptor field contribution for the WT and K103N inhibition are shown in Figures 12a and 12b, respectively. According to WT inhibition, a prominent orange contour is presented in the region of R substituent attached to the C4 site suggesting the preference of hydrogen bond acceptors at the position. It is in agreement with the observation that compounds containing acetylenic sidechain as the R substituent possessing hydrogen acceptor property, generally enhance the inhibitory activities. Compounds having alkoxy groups rather than

acetylenic sidechain at the R substituent show moderate to less binding affinities. An orange contour close to the carbonyl oxygen of the benzoxazin-2-one ring reveals that acceptor functions of the ligand directing to the location would be preferable for the binding affinity. This suggestion is in consistent with the obtained docking results described previously. Similar to the contribution obtained from the WT inhibition, a large orange contour corresponding to the location of the R group substituted to the C4 position shown in Figure 12b, suggests that hydrogen bond acceptors at the position could be beneficial for K103N binding affinity. Based on the obtained CoMSIA results, it could be confirmed that not only steric and electrostatic interactions contribute to the WT and K103N inhibitory activities, hydrophobic, hydrogen donor and acceptor fields are important to explain the variance of the data.

As the availability of the crystal structure of efavirenz complexed with HIV-1 RT [25,26], there are numerous contacts involving a series of hydrophobic contacts; the aromatic sidechains of Y181, Y188, W229 and F227 in the binding pocket with the bound inhibitor. The hydrogen bond between the benzoxain-2-one NH and the mainchain carbonyl oxygen of K101 is formed. There is also a Van der Waals contact between the γ-C of the sidechain of K103 and the nitrogen of benzoxain-2-one ring of efavirenz. An analysis of the structure of efavirenz complexed with the K103N RT reveals that the substitution of a charged and linear lysine for the uncharged and branched asparagine at the position 103 resulting in a drastic change in the chemical environment in the proximity of the mutation and a significant conformational rearrangement within the drug binding pocket compared with the wild type complex. Mainly, there are two consequences for the binding of NNRTI: changed hydrophobic and electrostatic properties of the binding pocket. It is evident that favorable

hydrophobic interactions of the amino acid in the binding pocket with the bound inhibitors and the hydrogen bond interaction are eliminated. Accordingly, the inhibitory affinities of some inhibitors are drastically reduced. Based on the obtained results, it could be suggested the methoxy group attached to the C5 position could be possible to generate favorable interactions compensating the hydrophobic interactions lost. The presence of NH group as the Z substituent in the benzoxazin-2-one ring possibly contributes to form the H-π interaction with the phenyl ring sidechain of Y181. The interactions should compensate the loss of significant interactions between the bound inhibitor and surrounding amino acid residues in the binding pocket. These results show high consistency to the obtained docking and CoMFA and CoMSIA models in the present study, highlighting the structural difference required for WT and K103N inhibitions of efavirenz derivatives.

Interaction Energy Calculations

Interaction energy of X-ray structure and docked efavirenz in the WT and K103N binding pockets

The interaction energies between efavirenz from the X-ray structure and each amino acid surrounding in the WT and K103N RT binding pockets are shown in Table 7. In the WT binding pocket, the interaction energies of efavirenz are -16.1 to 1.0 kcal/mol at the B3LYP/6-31G(d) level of theory. In case of interaction energies at the MP2/6-31G(d) levels of theory, all attractive interaction energies are obtained (-18.6 to -0.9 kcal/mol). Interaction energies from both levels of calculation shows in the same trend and the major attractive interaction is the interaction with K101 (-16.1 and -18.6 kcal/mol at the B3LYP/6-31G(d) and MP2/6-31G(d) levels of theory,

respectively. From the complex structure, amino and carbonyl groups of benzoxazin-2-one ring of efavirenz compound could form two H-bonding with carbonyl group (1.98 Å) and amino group (3.17 Å) of backbone K101, respectively. The interaction energies at the MP2/6-31G(d) levels of theory also reveal the important interaction of efavirenz to the WT binding pocket with L100, K103, Y181, Y188, H325, and P236.

For the K103N binding pocket, the interaction energies of efavirenz are -10.1 to 1.2 kcal/mol and -12.1 to -0.9 kcal/mol at the B3LYP/6-31G(d) and MP2/6-31G(d) levels of theory, respectively. Although K101 is the major attractive interaction of efavirenz in K103N binding pocket, the results clearly show the loss of attractive interaction with K101 about 5.0-6.5 kcal/mol, as compared with the WT binding pocket. Their interaction energies in the K103N binding pocket with K101 are -10.0 and -12.1 kcal/mol at the B3LYP/6-31G(d) and MP2/6-31G(d) levels of theory, respectively. Because of the effect of amide group at N103, the efavirenz position has slightly changed from the position in WT binding pocket and caused the longer H-bonding with carbonyl group of backbone K101. Amino and carbonyl groups of benzoxazin-2-one ring of efavirenz formed two H-bonding with carbonyl group (2.75 Å) and amino group (2.93 Å) of backbone K101, respectively. As compared to the interaction with K103 in the WT binding pocket, the interaction energies to N103 are decreased about 0.4 and 2.1 kcal/mol at the B3LYP/6-31G(d) and MP2/6-31G(d) levels of theory, respectively. These may cause from the loss of H-bonding between sidechain K103 between the WT binding pocket and efavirenz. For the interaction with other amino acids in the K103N binding pocket, the interaction energies are about ± 1 kcal/mol in both levels of theory as compared with those in the WT binding pocket.

In order to investigate the interaction energies of the docked conformation of other efavirenz derivatives, the interaction energies of docked efavirenz (compound.1) in WT and K103N binding pockets are firstly studied in comparison to those of X-ray structure. The interaction energies of compound 1 with the WT and K103N binding pockets are shown in Table 8 and Table 9, respectively. For the WT binding pocket, the interaction energies of compound 1 are -17.1 to 0.9 kcal/mol and -19.9 to -0.9 kcal/mol at the B3LYP/6-31G(d) and MP2/6-31G(d) levels of theory, respectively. Except K103, the interaction energies of compound 1 with other amino acids from both levels of theory are similar to those of X-ray structure with ± 1.5 kcal/mol. The interaction energies between compound 1 and K103 are more attractive than X-ray structure and K103 which the different of interaction energies are 3.6 and 2.9 kcal/mol at the B3LYP/6-31G(d) and MP2/6-31G(d) levels of theory, respectively. This more attractive interaction is caused from the stronger attractive interaction formed between fluoro atom of trifluoro group in efavirenz and γ-C of sidechain K103. The distances are 3.81 Å and 3.51 Å in X-ray structure and compound 1, respectively. Because this substituted group (trifluoro group) does not vary in this study, more attractive interaction with K103 may occur to other efavirenz derivatives with the same trend. According to this explanation, compound 1 can be used to compare the interaction with other efavirenz derivatives. In case of compound 1 in the K103N binding pocket, the interaction energies are -7.3 to 4.6 kcal/mol and -10.3 to -1.3 kcal/mol at the B3LYP/6-31G(d) and MP2/6-31G(d) levels of theory, respectively. The interaction energy differences between X-ray and compound 1 are ±1.7 kcal/mol, except L100 and K101. Because of a little movement of compound no. 1 to form more attractive interaction with Y181, attractive interaction with L100

and K101 are lost about 1.8 and 2.7 kcal/mol at MP2/6-31G(d), respectively. More attractive interaction with Y181 could occur with other efavirenz derivatives in the same manner. Therefore, to determine the interaction energies of other docked efavirenz derivatives, compound 1, which is the docked conformation of efavirenz, is used to compare in the further step.

Interaction energy of compounds 25 and 12 in WT binding pocket

The individual interaction is also observed with the compounds 25 and 12, the highest and less WT activity, respectively. Their interaction energies compared with compound 1 are shown in Table 8. The interaction energies of compound 25 in WT binding pocket are -17.2 to 0.4 kcal/mol and -20.0 to -0.4 kcal/mol at the B3LYP/6-31G(d) and MP2/6-31G(d) levels of theory, respectively. As compared with compound 1, the results confirm the docking results that slightly more attractive interaction to compound 25 could be formed to L100, K101, Y188, G190, and H235 with ±1.0 kcal/mol from both levels of theory. K103 and V106 are formed more attractive interactions within 2.0 kcal/mol. More attractive interaction with V106 is formed with the 5-F of the ring and this cause a slight shift of the fluoromethyl group to come closer to K103. For the less WT activity compound, interaction energies of compound 12 are -15.3 to 3.6 kcal/mol and -18.0 to -0.8 kcal/mol the B3LYP/6-31G(d) and MP2/6-31G(d) levels of theory, respectively. The decreased attractive interaction, as compared with compound 1, is found between compound 12 and most amino acids. Because of the bulky group attached at R position, steric interaction occurs with L100, K101, and Y181. The individual interaction results

support and agree well with the experimental results that compounds 25 and 12 show higher and lower potency than compound 1, respectively.

Interaction energy of compound 50 and 22 in K103N binding pocket

In the case of the K103N RT binding pocket, compounds 50 and 22, the highest and less potency against K103N RT, respectively, are selected to study. Their interaction energies are shown in Table 9. The interaction action energies of compound 50 in K103N binding pocket are -14.8 to 0.8 kcal/mol and -17.3 to -1.1 kcal/mol at the B3LYP/6-31G(d) and MP2/6-31G(d) levels of theory, respectively. From both levels of theory, more attractive interaction has significantly formed to L100, K101, Y181, and Y188. The attached substituted groups in compound 50 cause more fit of its conformation in K103N binding pocket than compound 1. Stronger attractive interaction is also formed with L100 and K101. The nitrogen atom on the Z substituent of compound 50 make the attractive interaction increased. The $H-\pi$ interaction to the aromatic sidechain of Y181 could be formed. The methoxy group attached at C5-position of phenyl ring has fitted with the hydrophobic pocket consisting of V106, Y188, and L234. Most of other amino acids in the binding pocket also slightly form more attractive interaction with compound 50. For the less active compound against the K103N RT, the interaction energies of compound 22 are -6.9 to 2.8 kcal/mol and -9.8 to -0.7 kcal/mol at the B3LYP/6-31G(d) and MP2/6-31G(d) levels of theory, respectively. From their docked conformation, it can be seen that the substituting group at R-position has caused the steric effect with the pocket around R-position. From the interaction energies, this substituting group at R-position of compound 22 has caused the less attractive interaction with P95, Y188, W229, and

L234. The individual interaction results are in agreement with the experimental results that compounds 50 and 22 shows highest and less potency against the K103N RT, respectively.

Based on the calculated results, more attractive interaction are found by using the MP2/6-31G(d) level of theory, as compare with B3LYP/6-31G(d) level of theory. The obtained interaction energies agree well as compared with the results previously reported [36,54]. Therefore, to ensure that H- π interaction is included in the calculation, MP2 method should be appropriated applied in the study. The interaction energies could be helpful for understanding the individual interaction between ligand and the binding pocket and suggesting for the guideline of the new more potent inhibitor design.

CONCLUSION

The molecular docking calculations and 3D-QSAR analyses were successfully combined to investigate the interaction and the relationship between structural requirements of efavirenz derivatives for WT and K103N HIV-1 RT. The potential binding orientation of the inhibitors in the binding pockets could be identified, by using docking studies. The docking results provide additional insight into essential inhibitor-enzyme interactions for different types of wild type and mutant type of HIV-1 RT. Based on the docking conformations, the reliable and predictive CoMFA and CoMSIA models of efavirenz derivatives for the WT and K103N RT inhibition were derived. The QSAR models are successfully used to discriminate between the structural requirements for WT and K103N inhibitory activities. Moreover, the interaction energy trend calculated from quantum chemical calculations of the

inhibitors and individual amino acid residues in the binding pockets is informative to highlight particular ligand-receptor interaction in molecular level. The results derived from all approaches validate each other and agree well with the ligand-receptor complex interaction derived from the X-ray crystallographic data. Evidently, in the present study, molecular modeling with the combination of structure-based and ligand-based drug design approaches integrated with quantum chemical calculations has been proven as attractive and efficient tools for better understanding of the key structural element for enhancing the interaction between efavirenz compounds and the WT and K103N RT. Consequently, the obtained results enable to provide beneficial guidelines to design novel compounds with higher anti-HIV-1 RT activities against WT and K103N RT.

ACKNOWLEDGEMENTS

The authors thank Prof. Dr. Peter Wolschann for helpful discussion and continuously supports and Dr. Songwut Suramitr for his kind assistance and suggestion in computational details. The research grants provided by the Thailand Research Fund (MRG4880001 and BRG4780007) are gratefully acknowledged. We thank LCAC, the postgraduate on education and research in petroleum and petrochemical technology, the high performance computing centers of Kasetsart University, the National Electronics and Computer Technology (HPCC/NECTEC) and the computer center of the University of Vienna for providing computational resources.

REFERENCES

- 1. Arnold, E; Das, K; Yadav, PNS; Hsiou, Y; Boyer, PL; Hughes, SH. Targeting HIV Reverse Transcriptase for Anti-AIDS Drug Design. *Drug. Des. Disc.* 1996, 13, 29-47.
- 2. De Clercq, E. The Role of Nonnucleoside Reverse Transcriptase Inhibitors (NNRTI) in the Therapy of HIV-1 Infection. *Anti. Viral Res.* 1998, 38, 153-179.
- 3. Evans, DB; Brawn, K; Deibel, MR; Tarpley, WG; Sharma SK. A Recombinant Ribonuclease H Domain of HIV-1 Reverse Transcriptase that is Enzymatically Active. *J. Biol. Chem.* 1991, 266, 20583-20585.
- 4. Young, SD. Non-nucleoside Inhibitors of HIV-1 reverse Transcriptase. *Perspect. Drug Desc. Des.* 1993, 1, 181-192.
- 5. Richman, D; Shih, CK; Lowy, I; Rose, J; Prodanovich, P; Goff, S; Griffin, J. Human Immunodeficiency Virus Type 1 Mutants Resistant to Nonnucleoside Inhibitors of Reverse Transcriptase Arise in Tissue Culture. *Proc. Natl. Acad. Sci. U.S.A.* 1991, 88, 11241–11245.
- 6. Balzarini, J; Karlsson, A; Sardana, VV; Emini, EA; Camarasa, MJ; De Clercq, E. Human Immunodeficiency Virus 1 (HIV-1)-Specific Reverse Transcriptase (RT) Inhibitors may Suppress the Replication of Specific Drug-Resistant (E138K) RT HIV-1 Mutants or Select for Highly Resistant (Y181C–.C181I) RT HIV-1 Mutants. *Proc. Natl. Acad. Sci. U.S.A.* 1994, 91, 6599–6603.

7. De Clercq, E. Non-nucleoside Reverse Transcriptase Inhibitors (NNRTI) for the Treatment of Human Immunodeficiency Virus Type 1 (HIV-1) Infections: Strategies to

Overcome Drug Resistance Development. Med. Res. Rev. 1996, 16, 125–157.

- 8. Ren, J; Esnouf, R; Garman, E; Somers, D; Ross, C; Kirby, I.; Keeling, J; Darby, G; Jones, Y; Stuart, D; Stammers, D. High Resolution Structures of HIV-1 RT from Four RT-Inhibitor Complexes. *Nat. Struct. Biol.* 1995, 2, 293–302
- 9. Ding, J; Das, K; Moereels, H; Koymans, L; Andries, K; Janssen, PA; Hughes, SH; Arnold, E. Structure of HIV-1 RT/TIBO R 86183 Complex Reveals Similarity in the Binding of Diverse Nonnucleoside Inhibitors. *Nat. Struct. Biol.* 1995, 2, 407–415.
- 10. Schinazi, RF; Larder, BA; Mellors, J. Mutations in Retroviral Genes Associated with Drug Resistance. *International Antiviral News*. 1997, *5*, 129–135.
- 11. Young, SD; et al., Emini, EA. L-743, 726 (DMP-266): A Novel, Highly Potent nonnucleoside Inhibitor of the Human Immunodeficiency Virus Type 1 Reverse Transcriptase. *Antimicrob. Agents Chemother*. 1995, 39, 2602–2605.
- 12. Bacheler, L; Wieslow, O; Snyder, S; Hanna, G; D'Aquila, R. The SUSTIVA Resistance Study Team. *Abstract, presented at the 12th World AIDS Conference, Geneva, Switzerland.* 1998.
- 13. Bacherler, L; Jeffrey, S; Hanna, G; D'Aquila, R; Wallace, L; Logue, K; Cordova, B; Hertogs, K; Larder, B; Buckery, R; Baker, D; Gallagher, K; Scarnati, H; Tritch, R; Rizzo, C. Genotypic Correlate of Phenotypic Resistance to Efavirenz in Virus Isolates

from Patients Failing Nonnucleoside Reverse Transcriptase Inhibitor Therapy. *J. Virol.* 2001, 75, 4999-5008.

14. Miller, V; Sturmer, M; Staszewski, S; Groschel, B; Hertogs, K; de Bethune, MP; Pauwels, R; Harrigan, PR; Bloor, S; Kemp, SD; Larder, BA. The M184V Mutation in HIV-1 Reverse Transcriptase (RT) Conferring Lamivudine Resistance does not Result in Broad Cross-resistance to Nucleoside Analogue RT Inhibitors. *AIDS*. 1998, 12, 705-712.

15. Torti, C; Pozniak, A; Nelson, M; Hertogs, K; Gazzard, BG. Distribution of K103N and/or Y181C HIV-1 Mutations by Exposure to Zidovudine and Non-nucleoside Reverse Transcriptase Inhibitors. *Antimicrob. Chemother*. 2001, 48, 113-116.

16. Patel, M; Ko, SS; McHugh, RJ; Markwalder, JA; Srivastana, AS; Cordova, BC; Klabe, RM; Erickson-Viitanen, S; Trainor, GL; Seitz, SP. Synthesis and Evaluation of Analogs Efavirenz (SUSTIVATM) as HIV-1 Reverse Transcriptase Inhibitors. *Bioorg. Med. Chem. Lett.* 1999, 9, 2805-2810.

17. Patel, M; McHugh, RJ; Jr.; Cordova, BC; Klabe, RM; Erickson-Viitanen, S; Trainor, GL; Ko, SS. Synthesis and Evaluation of Benzoxazinones as HIV-1 Reverse Transcriptase Inhibitors. Analogs of Efavirenz (SUSTIVATM). *Bioorg. Med. Chem. Lett.* 1999, 9, 3221-3224.

18. Patel, M; McHugh, RJ; Jr; Cordova, BC; Klabe, RM; Erickson-Viitanen, S; Trainor, GL; Rodgers, JD. Synthesis and Evaluation of Quinoxalinones as HIV-1 Reverse Transcriptase Inhibitors. *Bioorg. Med. Chem. Lett.* 2000, 10, 1729-1731.

- 19. Corbett, JW; Ko, SS; Rodgers, JD; Gearhart, LA; Magnus, NA; Bacheler, LT; Diamond, S; Jeffrey, S; Klabe, RM; Cordova, BC; Garber, S; Logue, K; Trainor, GL; Anderson, PS; Erickson-Viitanen, SK. Inhibition of Clinically Relevant Mutant Variants of HIV-1 by Quinazolinone Non-Nucleoside Reverse Transcriptase Inhibitors. *J. Med. Chem.* 2000, 43, 2019-2030.
- 20. Corbett, JW; Pan, S; Markwalder, JA; Cordova, BC; Klabe, RM; Garber, S; Rodgers, JD; Erickson-Viitanen, SK. 3,3a-Dihydropyrano[4,3,2,-de]quinazolin-2(1*H*)-ones are Potent Non-nucleoside Reverse Transcriptase Inhibitors. *Bioorg. Med. Chem. Lett.* 2001, 11, 211-214.
- 21. Markwalder, JA; Christ Abdul Mutlib, DD; Cordova, BC; Klabe, RM; Seitz, SP. Synthesis and Biological Activities of Potential Metabolites of the Non-nucleoside Reverse Transcriptase Inhibitor Efavirenz. *Bioorg. Med. Chem. Lett.* 2001, 11, 619-622.
- 22. Cocuzza, AJ; Chidester, DR; Cordova, BC; Jeffrey, S; Parsons, RL; Bacheler, LT; Erickson-Viitanen, S; Trainor, GL; Ko, SS. Synthesis and Evaluation of Efavirenz (SustivaTM) Analogues as HIV-1 Reverse Transcriptase Inhibitors: Replacement of the Cyclopropylacetylene Side Chain. *Bioorg. Med. Chem. Lett.* 2001, 11, 1177-1179.
- 23. Cocuzza, AJ; Chidester, DR; Cordova, BC; Klabe, RM; Jeffrey, S; Diamond, S; Weigelt, CA; Ko, SS; Bacheler, LT; Erickson-Viitanen, S; Rodgers, JD. 4,1-Benzoxazepinone Analogues of Efavirenz (SustivaTM) as HIV-1 Reverse Transcriptase Inhibitors. *Bioorg. Med. Chem. Lett.* 2001, 11, 1389-1392.

- 24. Patel, M; McHugh, RJ; Jr.; Cordova, BC; Klabe, RM; Bacheler, LT; Erickson-Viitanen, S; Rodgers, JD. Synthesis and Evaluation of Novel Quinoxalinones as HIV-1 Reverse Transcriptase Inhibitors. *Bioorg. Med. Chem. Lett.* 2001, 11, 1943-1945.
- 25. Ren, J; Milton, J; Weaver, KL; Short, SA; Stuart, DI; Stammers, DK. Structural Basis for the Resilience of Efavirenz (DMP-266) to Drug Resistance Mutations in HIV-1 Reverse transcriptase. *Structure*. 2000, 8, 1089-1094.
- 26. Lindberg, J; Sigurosson, S; Lowgren, S; Andersson, HO; Sahlberg, C; Noreen, R; Fridborg, K; Zhang, H; Unge, T. Structural Basis for Inhibitory Efficacy of Efavirenz (DMP-266), MSC194 and PNU142721 Towards the HIV-1 RT K103N Mutant. *Eur. J. Biochem.* 2002, 269, 1670-1677.
- 27. Hannongbua, S. Structural Information and Drug–Enzyme Interaction of the Non-Nucleoside Reverse Transcriptase Inhibitors Based on Computational Chemistry Approaches. *Top. Heterocycl. Chem.* 2006, 4, 55-84.
- 28. Udier-Blagovic, M; Watkins, EK; Tirado-Rives, J; Jorgensen, WL. Activity Predictions for Efavirenz Analogues with the K103N Mutant of HIV Reverse Transcriptase. *Bioorg. Med. Chem. Lett.* 2003, 13, 3337-3340.
- 29. Udier-Blagovic, M; Tirado-Rives, J; Jorgensen, WL. Structural and Energetic Analyses of the Effects of the K103N Mutation of HIV-1 Reverse Transcriptase on Efavirenz Analogues. *J. Med. Chem.* 2004, 47, 2389-2392.
- 30. Rodriguez-Barrios, F; Balzarini, J; Gago, F. The Molecular Basis of Resilience to the Effect of the Lys103Asn Mutation in Non-nucleoside HIV-1 Reverse

Transcriptase Inhibitors Studied by Targeted Molecular Dynamics Simulations. *J. AM. Chem. Soc.* 2005, 127, 7570-7578.

- 31. Weinzinger, P; Hannongbua, S; Wolschann, P. Related Articles, Links Molecular Mechanics PBSA Ligand Binding Energy and Interaction of Efavirenz Derivatives with HIV-1 Reverse Transcriptase. *J. Enzyme. Inhib. Med.* Chem. 2005, 20, 129-34.
- 32. Barreca, ML; Rao, A; Luca, LD; Zappala, M; Monforte, AM; Maga, G; Pannecouque, C; Balzarini, J; Clercq, ED; Chimirri, A; Monforte, P. Computational Strategies in Discovering Novel-nucleoside Inhibitors of HIV-1 RT. *J. Med. Chem.* 2005, 48, 3433-3437.
- 33. D'Cruz, OJ; Uckun, FM. Novel tight binding PETT, HEPT and DABO-based non-nucleoside inhibitors of HIV-1 reverse transcriptase. *J. Enzyme Inh. and Med. Chem.* 2006, 21, 329-350.
- 34. Xie, Q; Tang, Y; Li, W; Wang, HX; Qiu ZB. Investigation of the Binding Mode of (-)-Meptazinol and Bis-Meptazinol Derivatives on Acetylcholinesterase Using a Molecular Docking Method. *J. Mol. Model.* 2006, 12, 390-397.
- 35. Rawal, RK; Kumar, A; Siddiqi, MI; Katti, SB. Molecular Docking Studies on 4-Thiazolidinones as HIV-1 RT Inhibitors. *J. Mol. Model.* 2007, 13, 155–161.
- 36. Saparpakorn, P; Hannongbua, S; Rognan, D. Design of Nevirapine Derivatives Insensitive to the K103N and Y181C HIV-1 Reverse Transcriptase Mutants. *SAR QSAR Environ Res.* 2006, 17, 183-94.

- 37. Pungpo, P; Saparpakorn, P; Wolschann, P; Hannongbua, S. Computer-Aided Molecular Design of Highly Potent HIV-1 RT Inhibitors: 3D QSAR and Molecular Docking Studies of Efavirenz Derivatives. *SAR and QSAR in Environmental Research*. 2006, 17, 353-370.
- 38. Zhang, ZM; Zheng, LD; Shen, J; Luo, X; Zhu, W; Hualiang, J. Towards Discovering Dual Functional Inhibitors Against Both Wild Type and K103N Mutant HIV-1 Reverse Transcriptases: Molecular Docking and QSAR Studies on 4,1-Benzoxazepinone Analogues. *J. Comp. Aided Mol. Des.* 2006, 20, 281–293.
- 39. D'Cruz, OJ; Uckun, FM. Novel Broad-Spectrum Thiourea Non-Nucleoside Inhibitors for the Prevention of Mucosal HIV Transmission. *Current HIV Research*. 2006, 4, 329-345.
- 40. Ragno, R; Artico, M; De Martino, G; La Regina, G; Coluccia, A; Di Pasquali, A; Silvestri, R. Docking and 3-D QSAR Studies on Indolyl Aryl Sulfones. Binding Mode Exploration at the HIV-1 Reverse Transcriptase Non-Nucleoside Binding Site and Design of Highly Active N-(2-Hydroxyethyl)carboxamide and N-(2-Hydroxyethyl) carbohydrazide Derivatives. *J. Med. Chem.* 2005, 48, 213-223.
- 41. Medina-Franco, JL; Rodriguez-Morales, S; Juarez-Gordiano, C; Hernandez-Campos, Al; Jimenez-Barbero, J; Castillo, R. Flexible Docking of Pyridinone Derivatives into the Non-Nucleoside Inhibitor Binding Site of HIV-1 Reverse Transcriptase. *Bio. Med. Chem.* 2004, 12, 6085-6095.

- 42. Cramer, RD; Patterson, DE; Bunce, JD. Comparative Molecular Field Analysis (CoMFA). 1. Effect of Shape on Binding of steroids to Carrier Proteins. *J. Am. Chem. Soc.* 1988, 110, 5959-5967.
- 43. Klabe, G; Abraham, U; Mietzner, T. Molecular Similarity Indices in a Comparative Analysis (CoMSIA) of Drug Molecules to Correlate and Predict their Biological Activity. *J. Med. Chem.* 1994, 37, 4130-4146.
- 44. Kubinyi, H. 3D QSAR in Drug Design: Theory, Methods and Applications. ESCOM Science Publishers: Leiden. 1993.
- 45. Hannongbua, S; Nivesanond, K; Lawtrakul, L; Pungpo, P; Wolschann, P. 3D-Quantitative Structure-activity Relationships of HEPT Derivatives as HIV-1 Reverse Transcriptase Inhibitors, Based on Ab Initio Calculations. *J. Chem. Inf. Compul. Sci.* 2001, 41, 848-855.
- 46. Hannongbua, S; Pungpo, P; Wolschann, P. Quantitative Structure-activity Relationships and Comparative Molecular Field Analysis of the HIV-1 Reverse Transcriptase Inhibitor of TIBO Derivatives. *J. Comp. Aided Mol. Des.* 1999, 13, 563-577.
- 47. Pungpo, P; Hannongbua, S. Three-dimensional Quantitative Structure-activity Relationships Study on HIV-1 Reverse Transcriptase Inhibitors in the Class of Dipyridodiazepinone Derivatives, Using Comparative Molecular Field Analysis. *J. Mol. Grap. Mod.* 2000, 18, 581-590.

- 48. Zhang, H; Li, H; Liu, C. CoMFA, CoMSIA and Molecular Hologram QSAR Studies of Novel Neuronal nAChRs Ligands-Open Ring Analogues of 3-Pyridyl Ether. *J. Chem. Inf. Model.* 2005, 45, 440-448.
- 49. Barreca, ML; Carotti, A; Carrieri, A; Chimirri, A; Monforte, AM; Calace, MP; Rao, A. Comparative Molecular Field Analysis (CoMFA) and Docking Studies of Non-Nucleoside HIV-1 RT Inhibitors (NNIs). Bio. Med. Chem. 1999, 7, 2283-2292.
- 50. Chen, HF; Yao, XJ; Li, Q; Yuan, SG; Panaye, A; Doucet, JP; Fan, BT. Comparative Study of Nonnucleoside Inhibitors with HIV-1 Reverse Transcriptase Based on 3D-QSAR and Docking. *J. Comp. Aided Mol. Des.* 2003, 14, 455-474.
- 51. Medina-Franco, JL; Rodriguez-Morales, S; Juarez-Gordiano, C; Hernandez-Campos, A; Castillo, R. Docking-based CoMFA and CoMSIA Studies of Non-Nucleoside Reverse Transcriptase Inhibitors of the Pyridinone Derivative Type. *J. Comp. Aided. Mol. Des.* 2004, 18, 345-360.
- 52. Zhou, Z; Madura, JD. CoMFA 3D-QSAR Analysis of HIV-1 RT Nonnucleoside Inhibitors, TIBO Derivatives Based on Docking Conformation and Alignment. *J. Chem. Inf. Comput. Sci.* 2004, 44, 2167-2178.
- 53. Sea-oon, S; Kuno, M; Hannongbua, S. Binding Energy Analysis for Wild-Type and Y181C Mutant HIV-1 RT/8-Cl TIBO Complex Structures: Quantum Chemical Calculations Based on the ONIOM Method. *Proteins*. 2005, 61, 859-869.
- 54. Kuno, M; Hannongbua, S; Morokuma, K. Theoretical Investigation on Nevirapine and HIV-1 Reverse Transcriptase Binding Site Interaction, Based on ONIOM Method. *Chem. Phys Lett.* 2003, 380, 456-463.

- 55. Nunrium, P; Kuno, M; Saen-oon, S; Hannongbua, S. Particular Interaction between Efavirenz and the HIV-1 Reverse Transcriptase Binding Site as Explained by the ONIOM2 Method. *Chem. Phys. Lett.* 2005, 405, 198-202.
- 56. Bacheler, LT; Paul, M; Jadhav, PK; Otto, M; Miller, J. An Assay for HIV RNA in Infected Cell Lysates and Its Use for the Rapid Evaluation of Antiviral Efficacy. *Antiviral. Chem. Chemother.* 1994, 5, 111-121.
- 57. Alchemy 2000, Tripos Associates Inc. St., Louis. MO. 1998.
- 58. Frisch, MJ; Trucks, GW; Schlegel, HB; Gill, PMW; Jonhson, BG; Robb, MA; Cheeseman, JR; Keith, T; Petersson, GA; Montgomery, JA; Raghavachari, K; Al-Laham, MA; Zakrzewski, VG; Ortiz, JV; Foresman, JB; Peng, CY; Alaya, PY; Chen, W; Wong, WM; Andres, JL; Replogle, ES; Gomperts, R; Martin, RL; Fox, DJ; Binkley, JS; Defrees, DJ; Baker, J; Stewart, JP; Head-Gordon, M; Gonzales, C; Pople, JA. GAUSSIAN 94, Revision B.3, Gaussian, Inc. Pittsburgh PA. **1995**.
- 59. Jones, G; Wilett, P; Glen, RC; Leach, AR; Taylor, R. Development and validation of a genetic algorithm for flexible docking. *J. Mol. Biol.* 1997, 267, 727-748.
- 60. Morris, GM; Goodsell DS; Olson, AJ. The Scripps Research Institute, AutoDock 3.05, 2000.
- 61. SYBYL 7.0, Tripos Associates Inc., 1699 South Hanley Road, Suite 303, St. Louis, Missouri 63144, USA.
- 62. Viswanadhan, VN; Ghose, AK; Revenkar, GR; Robins, R. Atomic and Physichochemical Parameters for Three-dimensional Structure-directed Quantitative

Structure-activity Relationships. 4. Additional Parameters for Hydrophobic and Dispersive Interactions and Their Application for an Automated Superposition of Certain Naturally Occurring Antibiotics. *J. Chem. Inf. Comput. Sci.* 1989, 29, 163-172.

63. Klabe, G. The Use of Composite Crystal-field Environments in Molecular Recognition and the De Novo Design of Protein Ligands. *J. Mol. Biol.* 1994, 237, 212-235.

64. SYBYL Molecular Modeling Software, Version 6.3, SYBYL Ligand Base Design, Tripos Associates, Inc., St.Louis, Missouri 63144, USA, 1996, 299.

Table 1. Structures of 56 efavirenz derivatives and experimental biological activities against both WT RT and K103N RT

Compound	X	R	Z -	Experimental log(1/C)	
no.	Λ	K	L -	WT	K103N
01	6-Cl	CC-cyclopropyl	O	8.77	7.19
02	6-Cl	CC-2-pyridyl	O	8.27	5.96
03^{a}	6-Cl	CC-3-pyridyl	O	8.40	6.94
04	6-C1	CC-2-furanyl	O	8.42	6.82
05	6-C1	CC-3-furanyl	O	8.42	6.49
06	5,6-diF	CC-3-pyridyl	O	8.65	7.23
07	6-F	CC-3-furanyl	O	8.60	6.43
08	6-F	CC-3-pyridyl	O	8.59	6.48
09	5,6-diF	CC-3-furanyl	O	8.49	6.55

10	5,6-diF	CC-2-thienyl	O	8.65	6.81
11	5,6-diF	CC-3-thienyl	0	8.63	6.86
12	6-Cl	OCH ₂ CH ₂ CH ₂ CH ₃	O	7.99	6.00
13	6-C1	$OCH_2CH_2CH_2CH_3$ $OCH_2CH_2CH(CH_3)_2$	Ö	8.00	6.54
14	6-Cl	OCH ₂ CHCH(CH ₃)cis	O	8.36	6.63
15	6-Cl	OCH ₂ CHCH(CH ₃)tran	O	8.25	6.39
16	6-Cl	OCH ₂ CHC(CH ₃) ₃	O	8.57	7.08
17	6-Cl	OCH ₂ CCCH ₃	O	8.50	6.51
18	6-Cl	OCH ₂ CHCCl ₂	O	8.02	6.62
19 ^a	6-F	OCH ₂ CHC(CH ₃) ₂	O	8.53	6.97
20	6-F	OCH ₂ CHC(CH ₃) ₂	O	8.05	5.94
21	5,6-diF	OCH ₂ CHC(CH ₃) ₂	O	8.81	7.19
22 a	5,6-diF	OCH ₂ CHCH ₂	Ö	8.19	5.79
23	5,6-diF	OCH ₂ CHCCl ₂	Ö	8.20	6.74
24	5,6-diF	CC-ethyl	NH	8.82	7.85
25	5-F	CC-cyclopropyl	NH	8.85	7.05
26	5-Cl,6-F	CC-isopropyl	NH	8.52	7.82
27	5-Cl	CC-cyclopropyl	NH	8.60	7.2
28	5,6-diF	CC-cyclopropyl	NH	8.68	7.89
29	5,6-diF	CC-isopropyl	NH	8.68	7.85
30	6-F	CC-cyclopropyl	NH	8.70	7.32
31	5,6-diF	CC-2-pyridyl	NH	8.70	6.96
32	6-F	CC-ethyl	NH	8.60	7.15
33	5-Cl,6-F	CC-cyclopropyl	NH	8.57	7.74
34	6-MeO	CC-cyclopropyl	NH	8.54	7.4
35	6-F	CC-2-pyridyl	NH	8.30	6.32
36	5-F,6-Cl	CC-cyclopropyl	NH	8.32	7.74
37 ^a	5-Cl,6-F	CC-2-pyridyl	NH	8.64	7.14
38	6-Cl	CC-cyclopropyl	NH	8.57	7.66
39 a	6-MeO	CC-isopropyl	NH	8.42	7.25
40	6-MeO	CC-phenyl	NH	8.49	6.55
41	5,6-diF	CC-phenyl	NH	8.21	6.72
42 ^a	6-F	CC-phenyl	NH	8.18	6.49
43	6-Cl	CC-2-pyridyl	NH	8.47	6.8
44	6-Cl	CC-ethyl	NH	8.48	7.59
45	6-Cl	CC-phenyl	NH	8.15	6.6
46	6-F	CC-isopropyl	NH	8.59	7.57
47 ^a	5,6-diCl	CC-cyclopropyl	NH	8.10	7.74
48	6-Cl	CC-isopropyl	NH	8.52	7.66
49	6-MeO	CC-2-pyridyl	NH	8.09	6.47
50	5-MeO,6-Cl	CC-cyclopropyl	NH	8.46	8.12
51	5-MeO,6-Cl	CC-phenyl	NH	8.10	6.95
52	5-MeO,6-Cl	CC-3-pyridyl	NH	8.15	6.86
53	5-OH,6-Cl	CC-cyclopropyl	NH	8.44	7.55
54	6-Cl	CHCO-cyclopropyl	NH	8.44	7.12
55	6-Cl	CHCO-phenyl	NH	8.09	7.34
56	6-C1	CHCO-3-pyridyl	NH	8.34	7.12

Table 2. The rmsd (Å) of the docked pose from the X-ray pose of efavirenz by using GOLD and Autodock methods.

Doolsing mathed	Rmsd (Å)		
Docking method	WT (pdb code 1fk9)	K103N (pdb code 1fko)	
GOLD	0.94	1.00	
Autodock	0.35	0.53	

Table 3. Summary of CoMFA models for the WT and K103 N HIV-1 RT inhibition

Statistical results	WT inhibition	K103 N inhibition
r^2_{cv}	0.662	0.755
noc	3	6
s-press r ²	0.145	0.302
r^2	0.936	0.944
S	0.066	0.144
F	83.441	107.318
Field Contribution		
Steric	63.8	51.2
Electrostatic	36.2	48.8

Table 4. Summary of CoMSIA models for the WT and K103N HIV-1 RT inhibition

Statistical results	WT inhibition	K103 N inhibition
r^2_{cv}	0.708	0.773
noc	6	3
s-press	0.142	0.286
r^2	0.894	0.938
S	0.085	0.155
F	50.844	93.344
Field Contribution		
Steric	12.2	13.4
Electrostatic	19.5	22.3
Hydrophobic	24.1	20.5
Hydrogen donor	16.8	26.5

^a seven compounds comprising of compounds 03,19,22,37,39,42 and 47, used as the test set

Table 5. Predicted log (1/C) WT and K103N HIV-1 RT inhibitory affinities of the tested efavirenz compounds derived from CoMFA models

Compound	WT HIV-1 RT inhibitory affinity			K103N HIV-1 RT inhibitory affinity		
No.	Expt.log(1/C)	Calc.log (1/C) ^a	Residual	Expt.log(1/C)	Calc. $\log (1/C)^b$	Residual
03	8.40	8.50	-0.1	6.94	6.28	0.66
19	8.53	7.99	0.54	6.97	6.46	0.51
22	8.19	8.73	-0.54	5.79	7.42	-1.63
37	8.64	8.43	0.21	7.14	6.76	0.38
39	8.42	8.34	0.08	7.25	7.79	-0.54
42	8.18	8.27	-0.09	6.49	6.51	-0.02
47	8.10	8.63	-0.53	7.74	7.78	-0.04

^a calculated by CoMFA model for the WT inhibition

Table 6. Predicted log (1/C) WT and K103N HIV-1 RT inhibitory affinities of the tested efavirenz compounds derived from CoMSIA models

Compound No.	WT HIV-1 RT inhibitory affinity			K103N HIV-1 RT inhibitory affinity		
110.	Expt.log(1/C)	Calc.log (1/C) ^a	Residual	Expt.log(1/C	Calc. $\log (1/C)^b$	Residual
03	8.40	8.46	-0.06	6.94	6.58	0.36
19	8.53	8.27	0.26	6.97	6.23	0.74
22	8.19	8.58	-0.39	5.79	6.43	-0.64
37	8.64	8.20	0.44	7.14	6.72	0.42
39	8.42	8.54	-0.12	7.25	7.48	-0.23
42	8.18	8.23	-0.05	6.49	6.54	-0.05
47	8.10	8.47	-0.37	7.74	7.81	-0.07

^b calculated by CoMFA model for the K103N inhibition

Table 7. Interaction energies between efavirenz from X-ray structure and each amino acid surrounding in the WT and K103N binding pockets

	Interaction energy (kcal/mol)						
- Amino acid residue	WT bind	ding pocket	K103N bi	nding pocket			
_	B3LYP/ 6-31G(d)	MP2/6-31G(d)	B3LYP/ 6-31G(d)	MP2/6-31G(d)			
P95	-0.3	-0.9	-0.3	-0.9			
L100	-0.6	-7.6	0.2	-7.7			
K101	-16.1	-18.6	-10.1	-12.1			
K103/N103	-1.8	-5.3	-1.4	-3.2			
V106	1.0	-2.4	-0.1	-3.2			
Y181	-0.6	-3.8	1.2	-4.3			
Y188	-1.0	-5.7	-1.6	-6.6			
G190	-1.0	-1.7	-1.0	-1.9			
F227	0.1	-1.0	0.4	-1.0			
W229	-0.7	-2.5	-1.3	-3.3			
L234	0.2	-1.8	0.0	-2.5			
H235	-1.7	-3.2	-1.9	-3.0			

^a calculated by CoMSIA model for the WT inhibition

^b calculated by CoMSIA model for the K103N inhibition

P236	-0.9	-3.1	-1.1	-2.7
Y318	-0.3	-2.7	-0.2	-3.3

Table 8. Interaction energies between docked conformations (docked efavirenz (compound 01), compounds 25 and 12) and each amino acid surrounding in the WT binding pocket

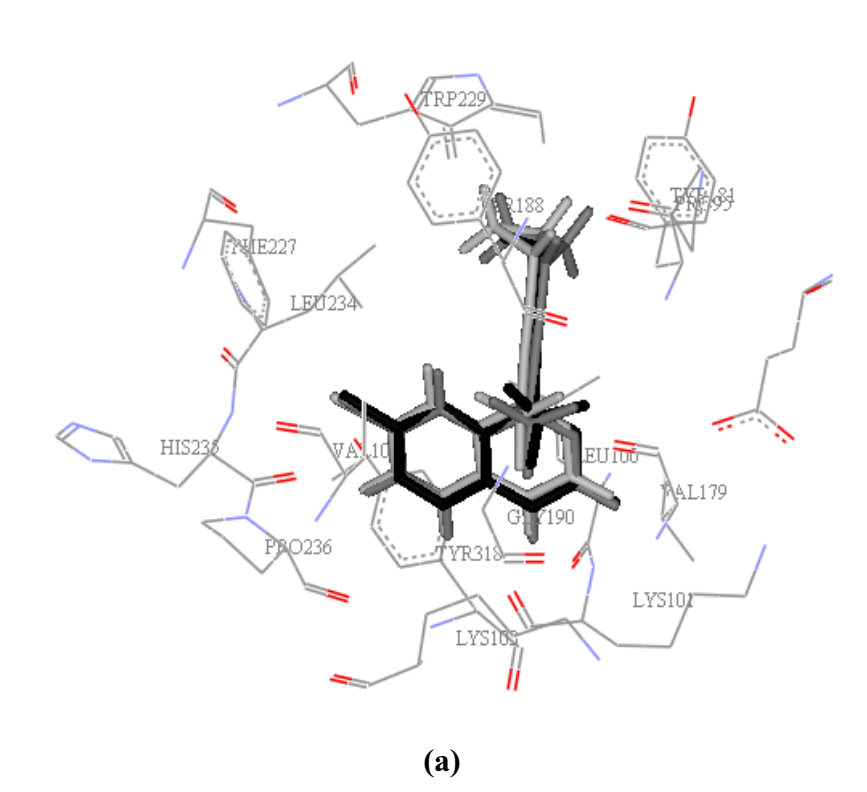
	Interaction energy (kcal/mol)						
Amino – acid residue –	compo	und 01	compo	und 25	compo	und 12	
	B3LYP/ 6-31G(d)	MP2/ 6-31G(d)	B3LYP/ 6-31G(d)	MP2/ 6-31G(d)	B3LYP/ 6-31G(d)	MP2/ 6-31G(d)	
P95	-0.1	-0.9	-0.1	-0.9	-0.3	-0.8	
L100	0.9	-6.3	0.4	-7.0	3.6	-3.2	
K101	-17.1	-19.9	-17.2	-20.0	-15.3	-18.0	
K103	-5.4	-8.2	-7.3	-10.2	-4.6	-7.7	
V106	0.7	-2.5	-1.7	-4.1	1.2	-2.2	
Y181	-0.1	-4.1	-0.1	-4.0	2.1	-1.9	
Y188	-0.7	-5.2	-1.2	-6.1	1.0	-4.6	
G190	-1.4	-2.1	-1.5	-2.3	-1.3	-2.3	
F227	-0.1	-1.1	0.0	-0.4	-0.2	-1.2	
W229	-1.4	-2.5	-0.4	-2.3	0.3	-2.5	
L234	0.2	-1.8	-0.1	-1.4	0.1	-1.8	

H235	-1.5	-2.9	-2.2	-3.0	-0.4	-2.0
P236	-1.4	-3.6	-0.8	-2.7	-1.2	-3.7
Y318	-0.3	-3.7	0.3	-3.4	0.1	-3.7

Table 9. Interaction energies between docked conformations (docked efavirenz (compound 01), compounds 50 and 22) and each amino acid surrounding in the K103N binding pocket

Amino – acid residue –	Interaction energy (kcal/mol)						
	compo	und 01	compo	und 50	compo	ound 22	
	B3LYP/ 6-31G(d)	MP2/ 6-31G(d)	B3LYP/ 6-31G(d)	MP2/ 6-31G(d)	B3LYP/ 6-31G(d)	MP2/ 6-31G(d)	
P95	-0.3	-1.3	-0.1	-1.1	-0.1	-0.7	
L100	4.6	-5.0	0.8	-7.8	2.8	-5.1	
K101	-7.3	-10.3	-14.8	-17.3	-6.9	-9.8	
N103	0.0	-1.5	0.3	-1.2	-0.1	-2.0	
V106	0.7	-2.0	0.3	-3.1	0.1	-3.0	
Y181	0.4	-5.9	-2.1	-8.9	1.5	-5.0	
Y188	-1.6	-5.1	-1.9	-7.5	-0.5	-4.1	
G190	-1.3	-2.2	-1.5	-2.5	-1.0	-2.0	
F227	-0.3	-1.3	0.7	-1.4	-0.4	-0.9	
W229	-1.0	-3.8	-1.1	-4.0	-0.7	-1.6	
L234	-0.2	-2.0	0.0	-2.9	0.3	-0.4	

H235	-1.5	-2.3	-1.9	-2.9	-1.7	-2.1
P236	-1.4	-2.6	-1.0	-2.5	-1.8	-3.1
Y318	0.3	-3.3	0.2	-3.4	0.0	-3.0



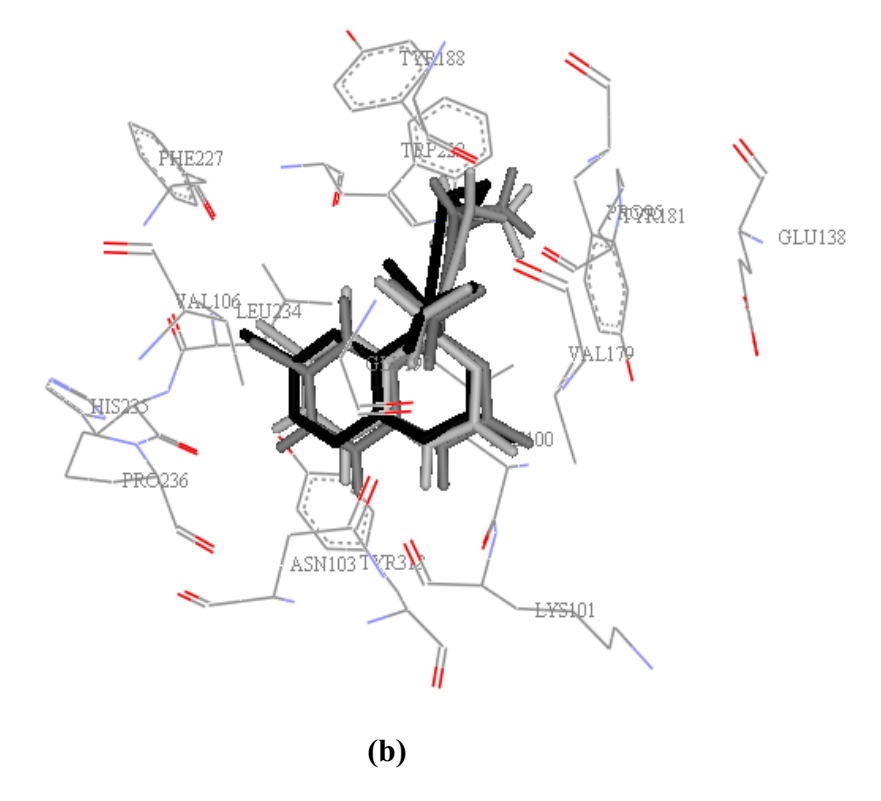
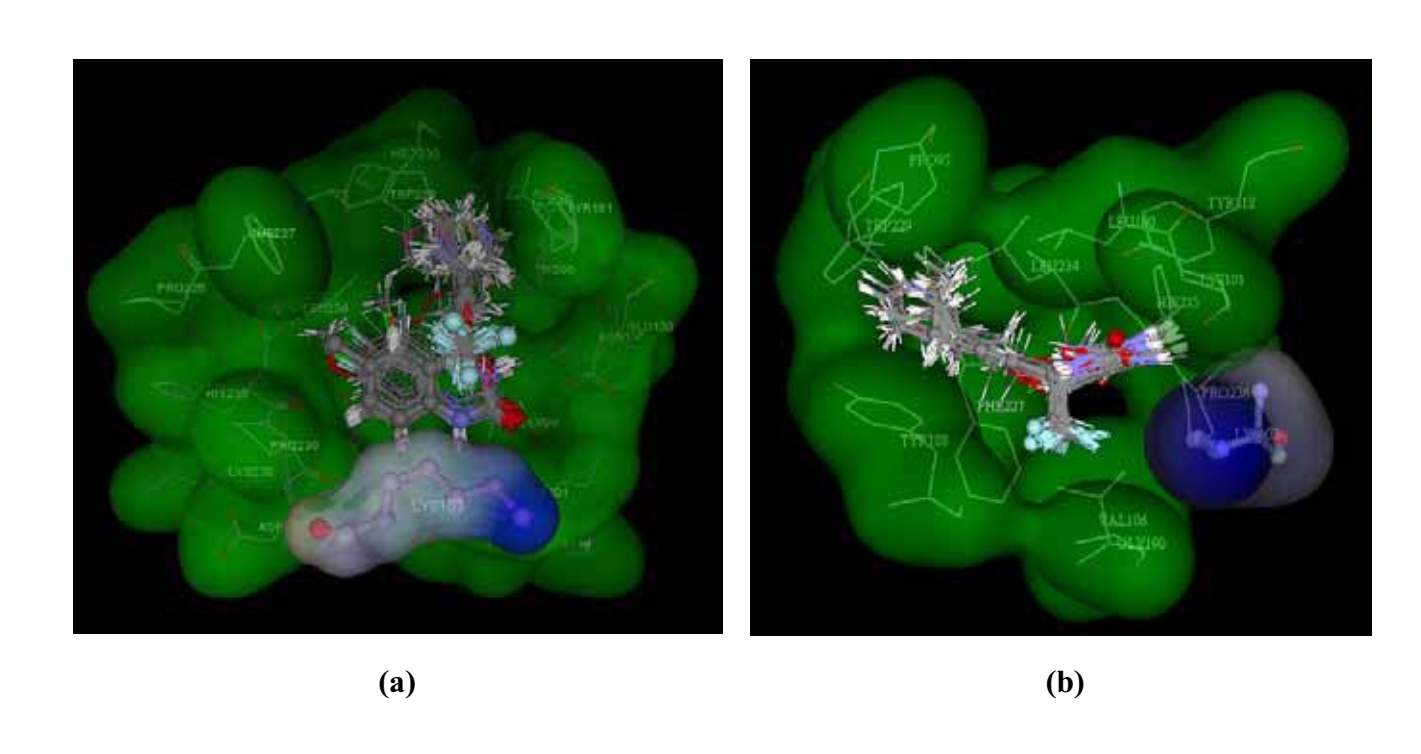


Figure 1. The conformations of docked efavirenz by using GOLD (grey) and Autodock (dark grey) and compared with the orientation of X-ray pose (black); (a) in the WT binding pocket (pdb code 1fk9) and (b) in the K103N binding pocket (pdb code 1fko).



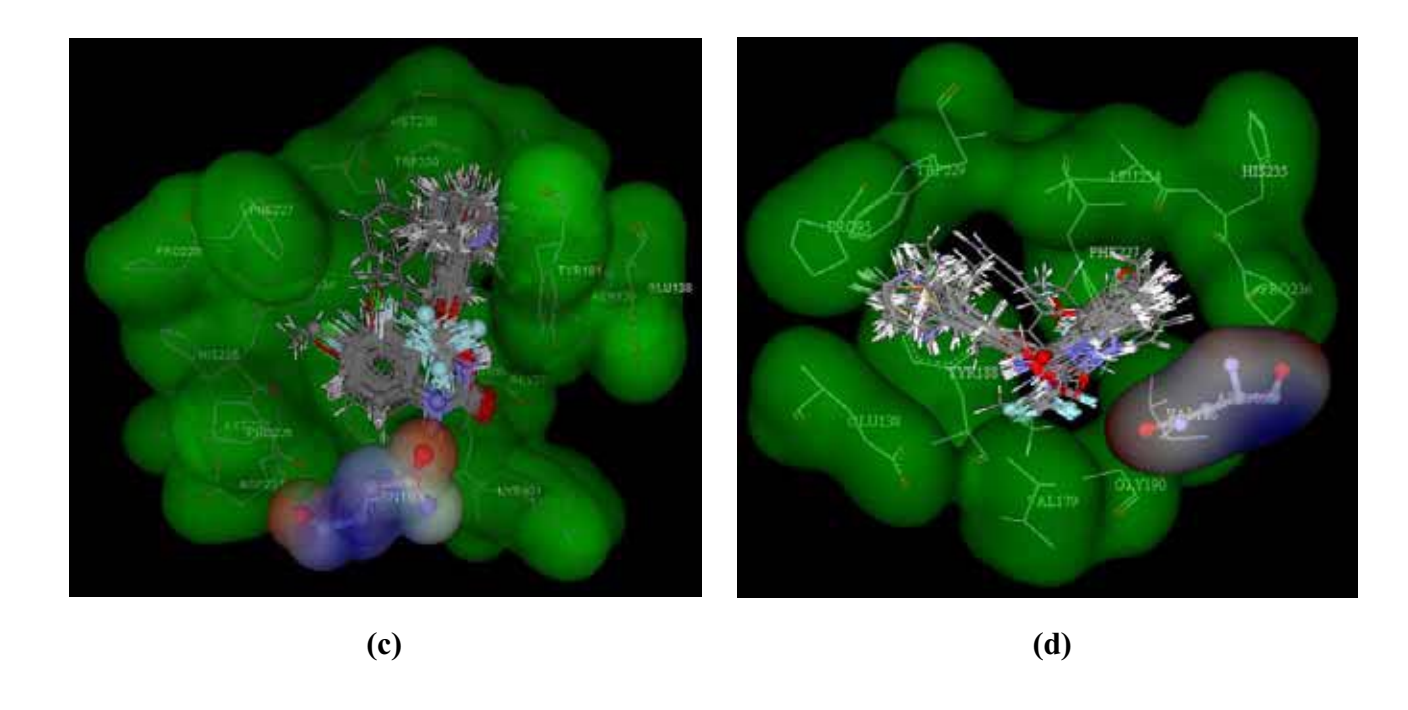
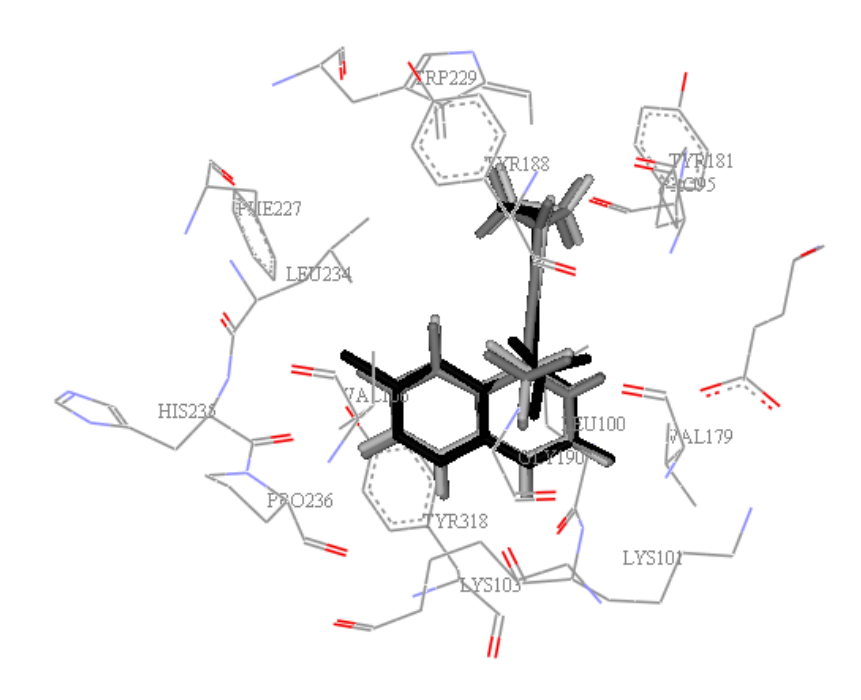


Figure 2. The orientation of docked efavirenz derivatives by using Autodock in the WT binding pocket (a. top view and b. side view) and in the K103N binding pocket (c. top view and d. side view).



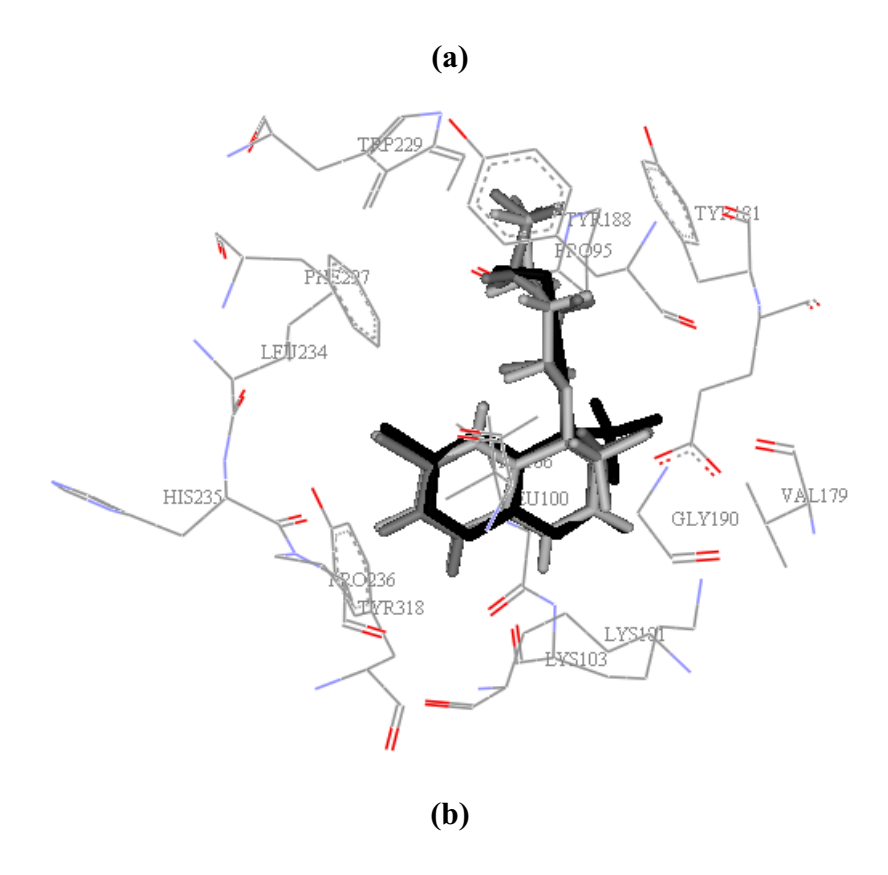


Figure 3. The conformations of docked efavirenz derivatives by using GOLD (grey) and Autodock (dark grey) and compared with the orientation of X-ray pose (black) in the WT HIV-1 RT; (a) Compound 25 and (b) Compound 12.

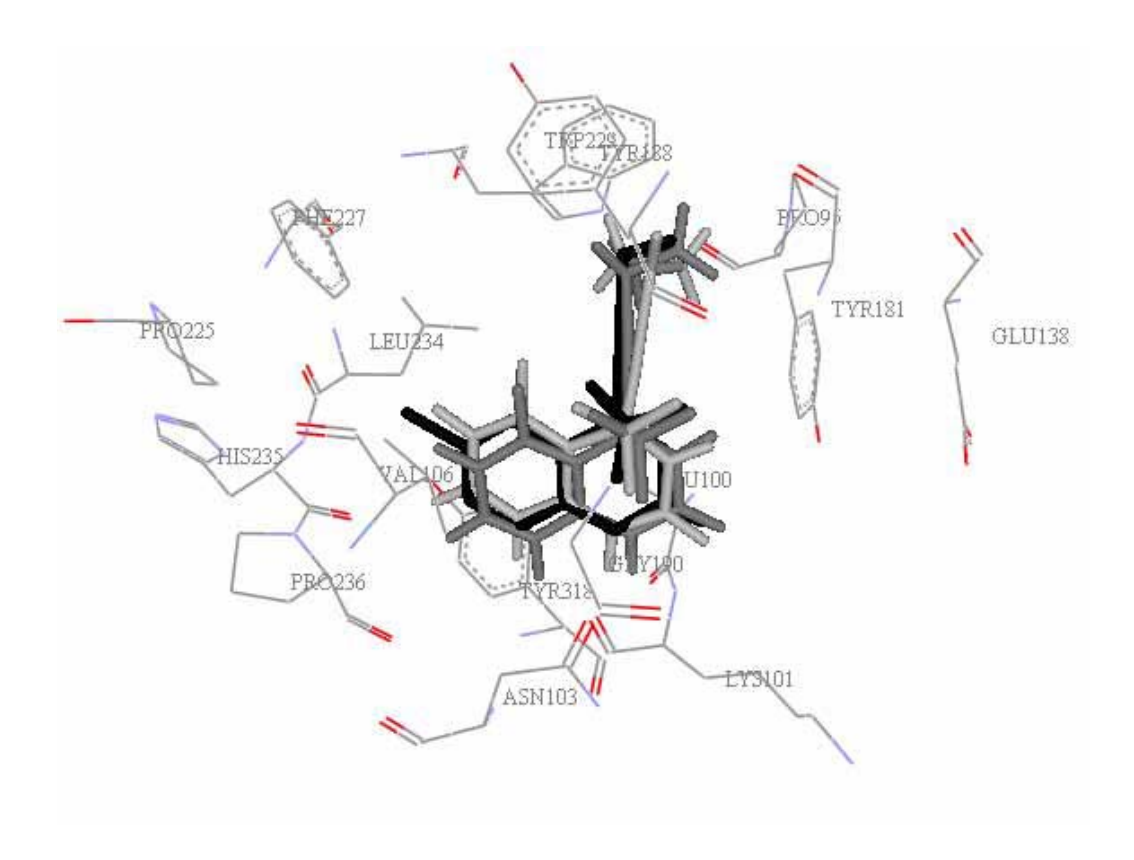


Figure 4. The conformations of docked efavirenz derivative (compound 25) by using GOLD (grey) and Autodock (dark grey) compared with the orientation of X-ray pose (black) in the K103N HIV-1 RT.

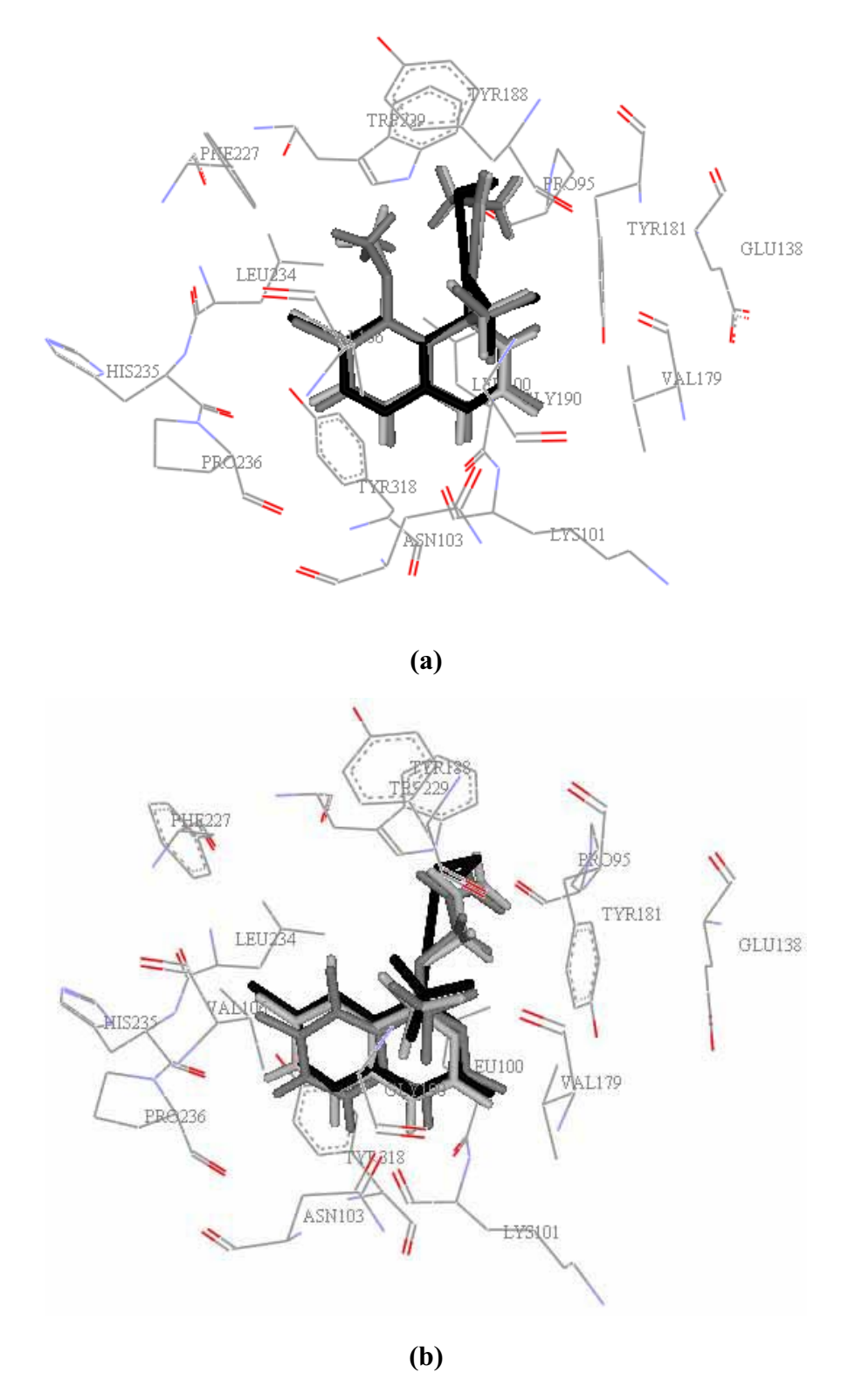


Figure 5. The conformations of docked efavirenz derivatives by using GOLD (grey) and Autodock (dark grey) compared with the orientation of X-ray pose (black) in the K103N HIV-1 RT; (a) Compound 50 (b) Compound 22.

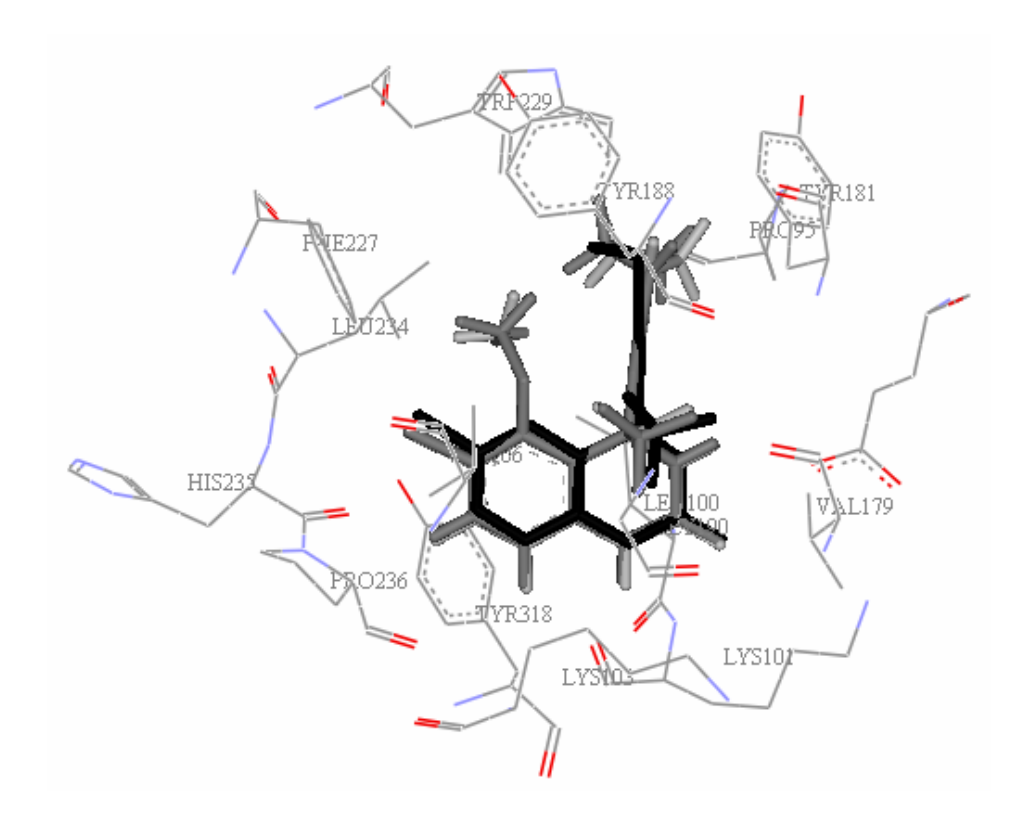


Figure 6. The conformations of docked efavirenz derivative (compound 50) by using GOLD (grey) and Autodock (dark grey) compared with the orientation of X-ray pose (black) in the WT HIV-1 RT.

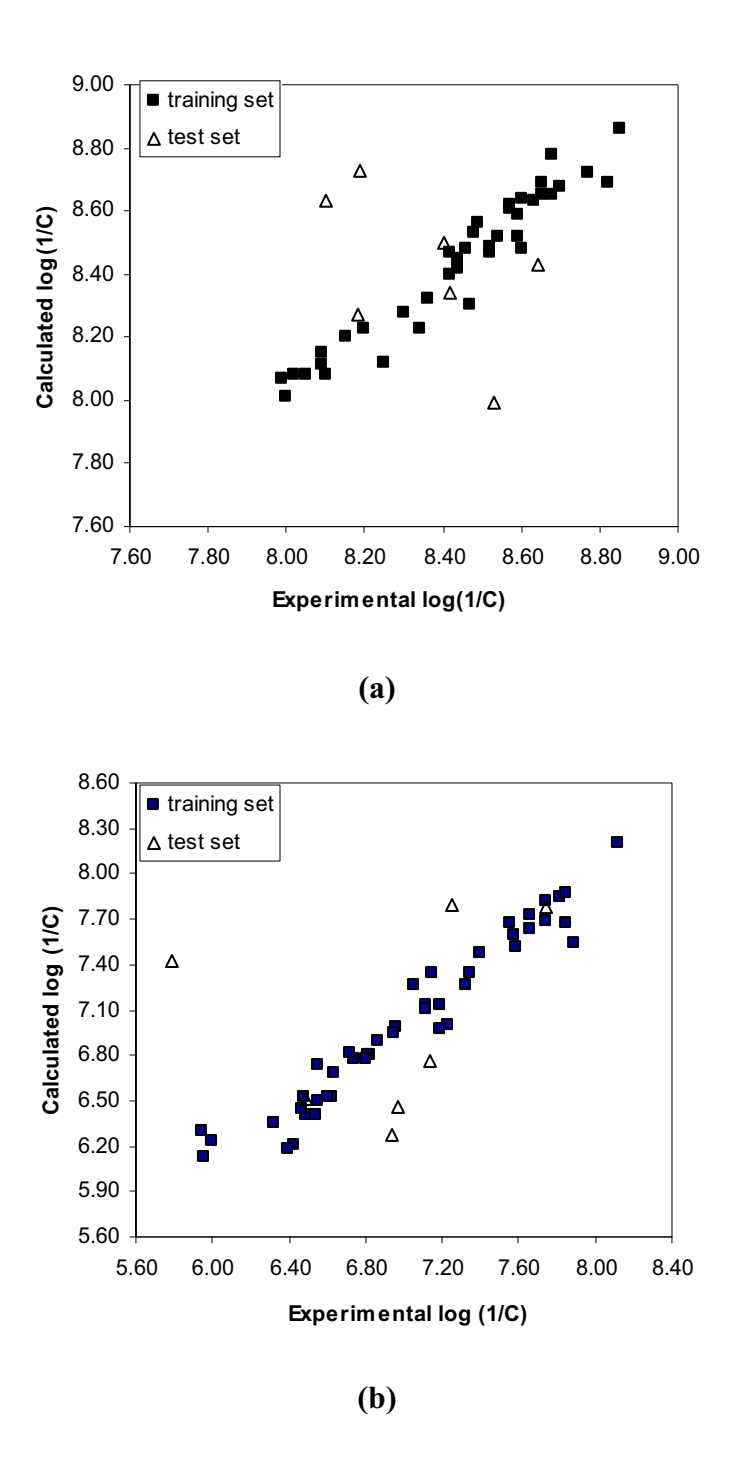


Figure 7. The plots between predicted and experimental inhibitory affinities of the non-cross-validated analysis of the CoMFA model; (a) WT inhibitory affinities and (b) K103N inhibitory affinities.

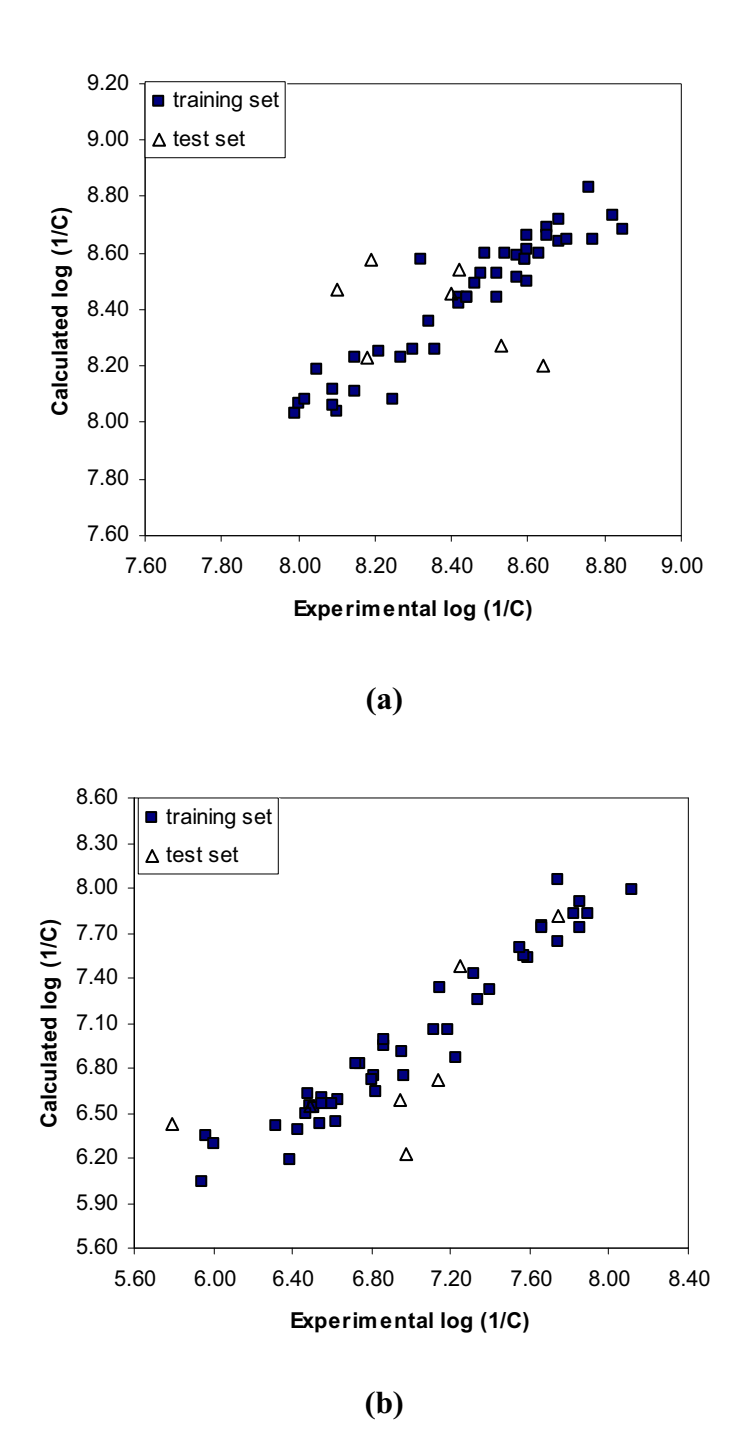
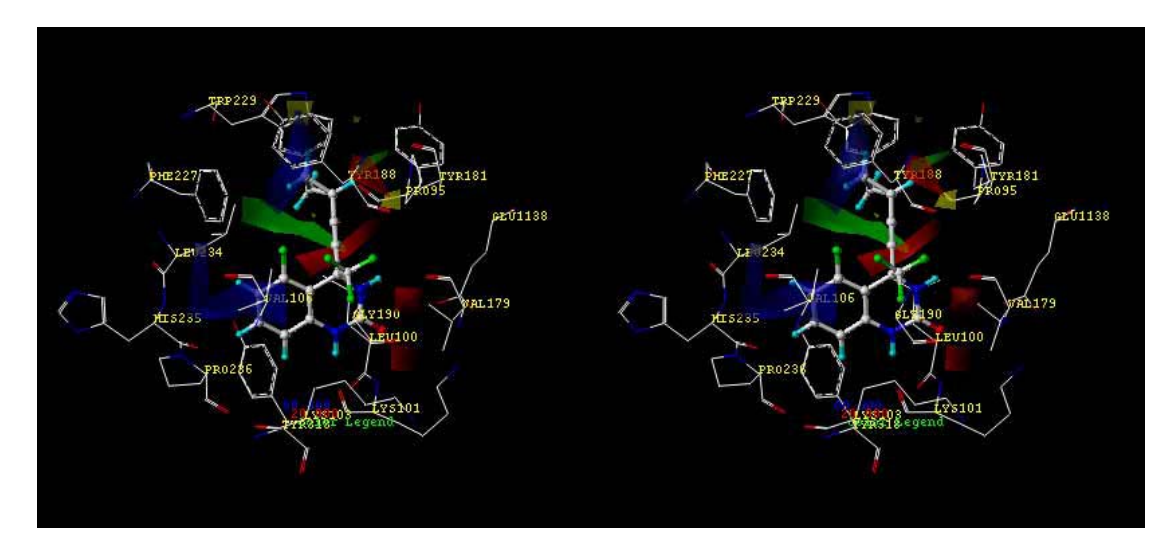


Figure 8. The plots between predicted and experimental inhibitory affinities of the non-cross-validated analysis of the CoMSIA model; (a) WT inhibitory affinities and (b) K103N inhibitory affinities.



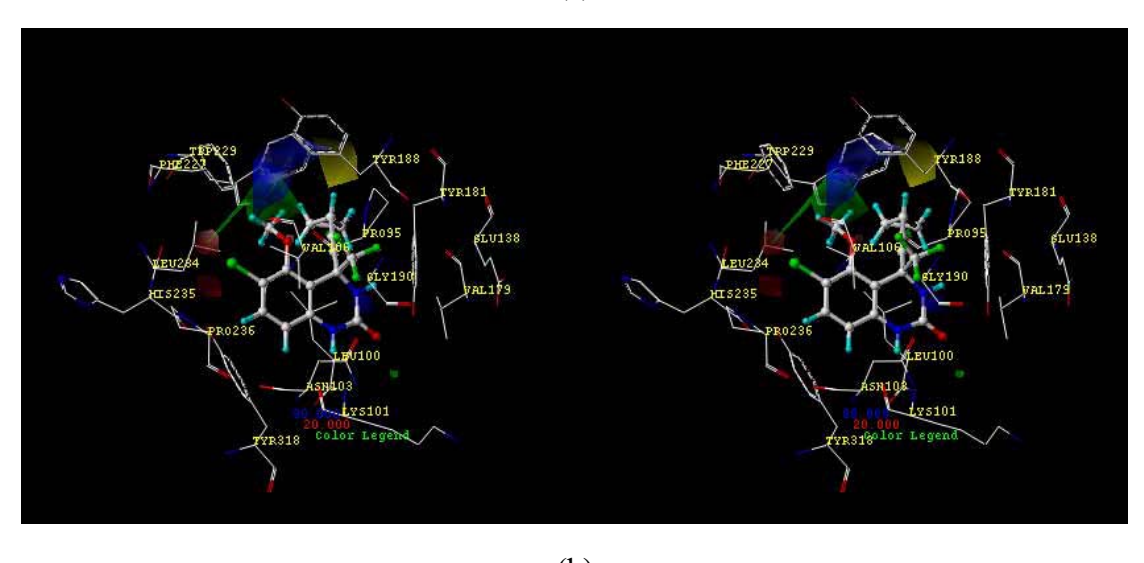
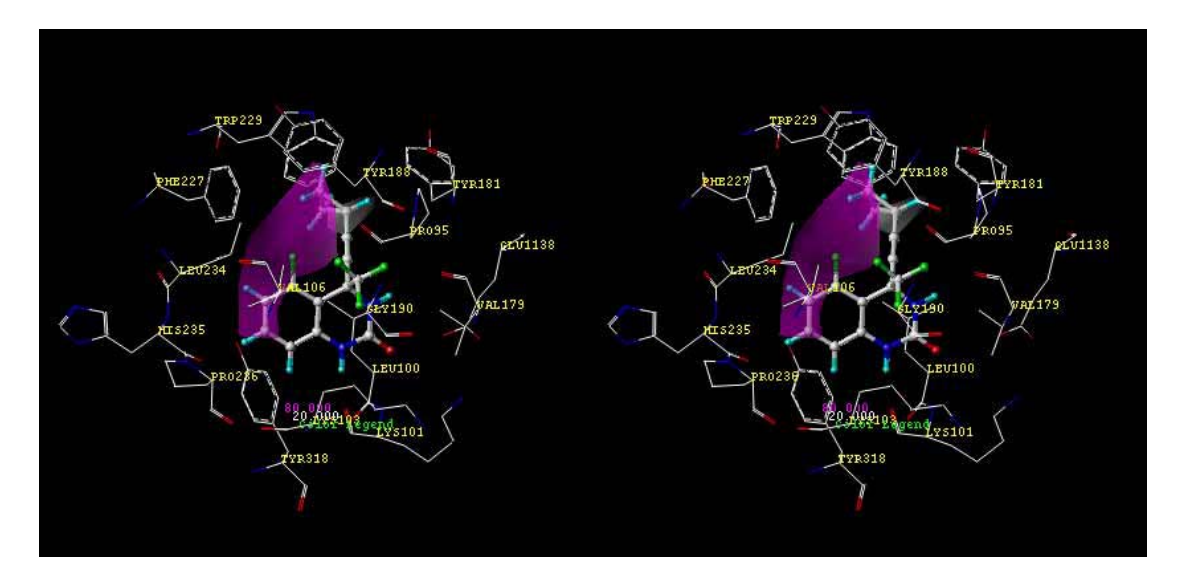


Figure 9. Stereoview of CoMFA steric and electrostatic STDEV*COEFF contour plots based on WT and K103N HIV-1 RT inhibitions from the analysis of CoMFA models with non-cross-validation, as shown in (a) and (b), respectively. Green contours refer to sterically favored regions; yellow contours indicate disfavored area. Compound 25 and 50 are displayed inside the fields as ball and stick presentation in (a) and (b), respectively.



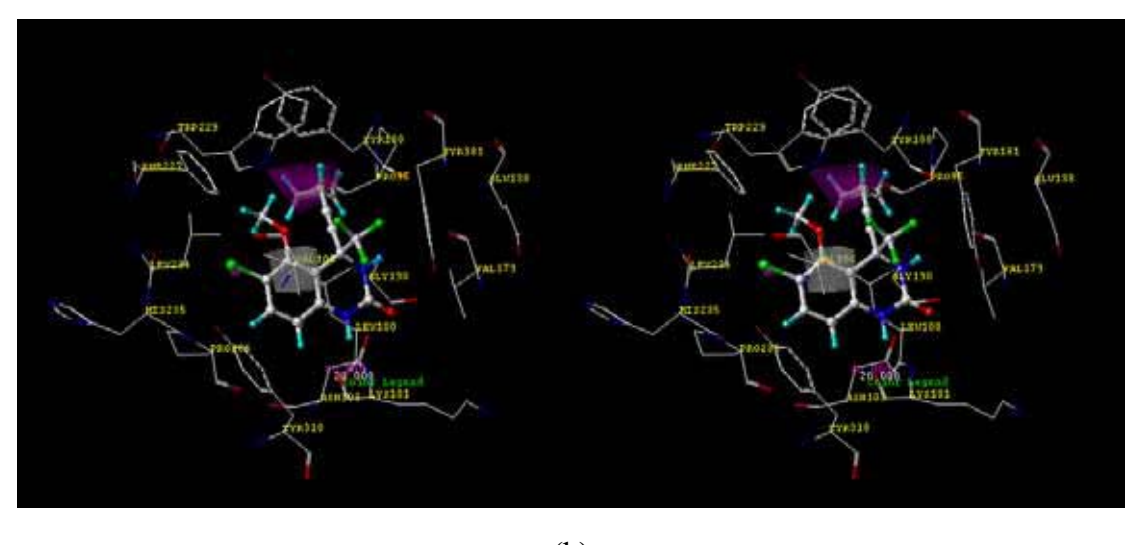
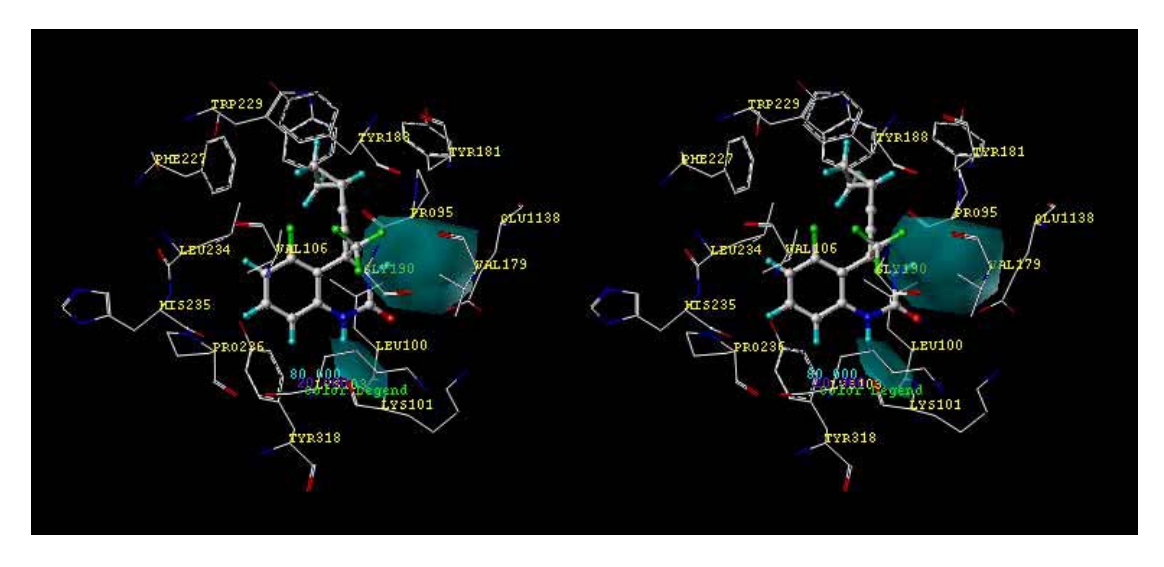


Figure 10. Stereoview of CoMSIA hydrophobic STDEV*COEFF contour plots based on WT and K103N HIV-1 RT inhibitions from the analysis of CoMSIA models with non-cross-validation, as shown in (a) and (b), respectively. Magenta contours refer to positive hydrophobic favoring areas; white contours indicate hydrophilic favoring areas. Compound 25 and 50 are displayed inside the fields as ball and stick presentation in (a) and (b), respectively.



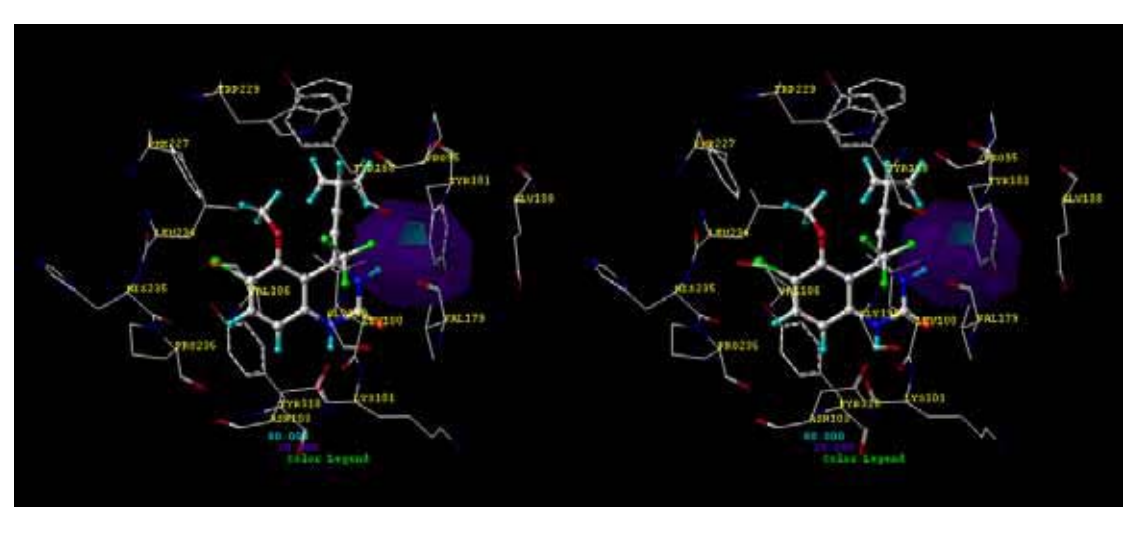
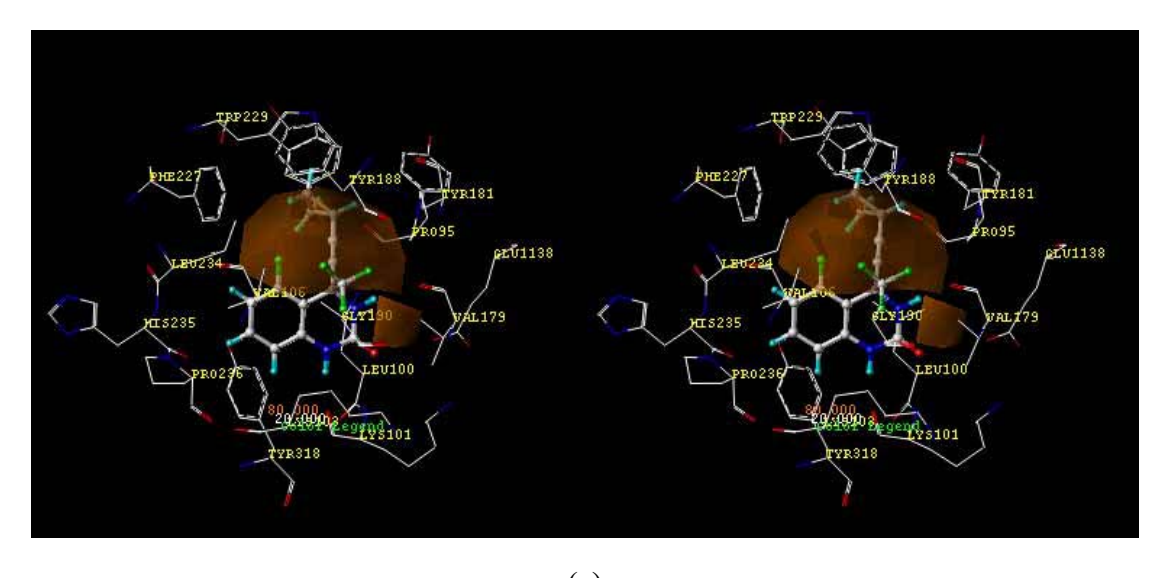


Figure 11. Stereoview of CoMSIA hydrogen donor STDEV*COEFF contour plots based on WT and K103N HIV-1 RT inhibitions from the analysis of CoMSIA models with non-cross-validation, as shown in (a) and (b), respectively. Cyan contours refer to hydrogen donor fields favoring areas; purple contours indicate hydrogen donor fields disfavoring areas. Compound 25 and 50 are displayed inside the fields as ball and stick presentation in (a) and (b), respectively.



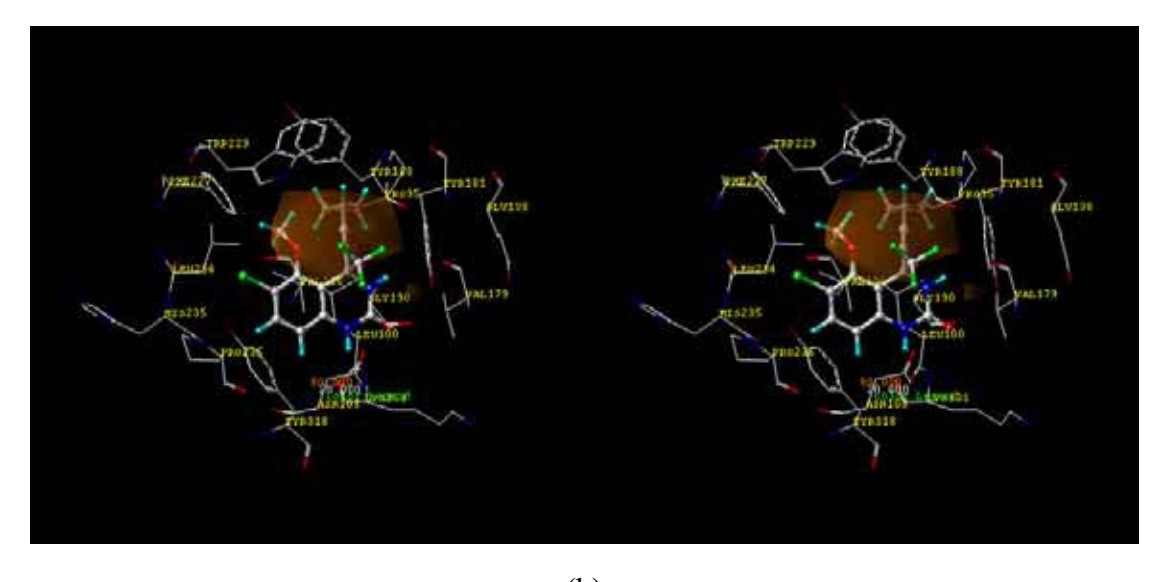


Figure 12. Stereoview of CoMSIA hydrogen acceptor STDEV*COEFF contour plots based on WT and K103N HIV-1 RT inhibitions from the analysis of CoMSIA models with non-cross-validation, as shown in (a) and (b), respectively. Orange contours refer to hydrogen acceptor fields favoring areas; white contours indicate hydrogen acceptor fields disfavoring areas. Compound 25 and 50 are displayed inside the fields as ball and stick presentation in (a) and (b), respectively.

Structural Aspects of Non-Nucleoside HIV-1 Reverse Transcriptase Inhibition

Anton Beyer*1, Luckhana Lawtrakul2, Pornpan Pungpo3 and Peter Wolschann1

Abstract: HIV-1 Reverse transcriptase (RT) is an essential enzyme for HIV-1 replication and, therefore, it is an important target for the attack of antiviral agents. Although some products are already on the market, there is need to design new drugs, because mutation in drug interacting disease proteins decreases the efficiency of the existing drugs. Non-nucleoside RT inhibitors fill up an allosteric, mainly hydrophobic pocket in a distinct distance from the enzyme's active center. X-ray crystallographic investigations on the enzyme and on enzyme complexes provide information about the structural consequences of the protein-inhibitor interaction. Applying molecular simulations the dynamic behaviour of these biomolecular systems can be obtained in order to get some insight into the molecular flexibilities and into the detailed inhibition mechanism. Amino acids which are important for the inhibition mechanism and the interaction with inhibitor molecules can be identified for further considerations with more accurate molecular calculations. QSAR studies allow the development of proper prediction models, which are used to design new drugs. Combination of molecular docking, energy minimization and MD or MC calculations with various QSAR methods will support screening methods to find new lead compounds.

Keywords: HIV-1 reverse transcriptase, Non-nucleoside reverse transcriptase inhibitor, X-ray structures, quantitative structure-activity analysis, molecular simulation.

1. STRUCTURE OF HIV-1 REVERSETRANSCRIPTASE AND INHIBITOR COMPLEXES

1.1 The Enzymes of HIV-1

The human immunodeficiency virus type 1 (HIV-1) is a retrovirus responsible for the Acquired Immunodeficiency Syndrome (AIDS). The viral genome (GenBank Accession number NC_001802) consists of 9181 base pairs and encodes nine open reading frames. One of these encodes the Pol polyprotein, which is proteolyzed into three enzymatic proteins, reverse transcriptase (RT), protease (PR) and integrase (IN) [1,2]. These enzymes are essential for the replication of the virus and therefore for the whole viral life cycle. After absorption of the virus by the cell, the RT converts the singlestranded viral RNA into double-stranded DNA, which is then integrated into the host chromosome by the IN. The polyprotein expressed from the resulting cellular RNA is cut into the individual proteins by the PR. These viral enzymes are important targets for the treatment of HIV-1 infection. Several products are already on the market [3-7], especially for the inhibition of the two enzymes PR and RT.

1.2. HIV-1 Reverse Transcriptase

HIV-1 RT is a multifunctional enzyme that converts the viral RNA into DNA and has the following functions: RNA-dependent DNA polymerase, DNA-dependent DNA polymerase and ribonuclease H (RNase H). Chain elongation takes place by adding desoxyribonucleotide triphosphates to the 3'OH terminus of the primer sequence. This process is essential for the replication of HIV-1, and the enzyme is therefore an

important target for anti-HIV-1 drugs [8-10]. Three classes of inhibitors exist, acting on HIV-1 RT. Nucleoside Reverse Transcriptase Inhibitors (NRTIs) and Nucleotide Reverse Transcriptase Inhibitors (NtRTIs), which interact with the enzyme's active site and are competitive inhibitors. Nonnucleoside inhibitors (NNRTIs) are the third class of RT inhibitors. They act allosterically and are highly specific for HIV-1 RT. NNRTIs are compounds of a surprisingly different chemical constitution, and all bind to the same site of RT, near to, but distinct from the polymerase active center. They inhibit the RT activity by inducing conformational changes at functionally important residues.

A major drawback of NNRTIs is the occurrence of drug resistance by mutation of the RT protein [11-13]. Additionally, such mutations in many cases also lead to a decreased sensitivity to other NNRT inhibitors. This is the reason for the necessity of the development of new and more mutation-independent drugs.

1.3. Structure of HIV-1 Reverse Transcriptase

Extended structural information about HIV-1 RT has been obtained from X-ray crystallography. A large number of structures of free or complexed HIV-1 RT, resolved by X-ray crystallography, have been deposited in the Protein Data Bank (RCSB PDB; http://www.pdb.org) [14]. The following classes of structures are included in the data bank: Free HIV-1 RT without ligand, HIV-1 RT bound to double-stranded oligonucleotide template-primers both in the presence and in the absence of a deoxynucleotide triphosphate substrate and HIV-1 RT complexed with different NNRTIs. Moreover, Structures of HIV-1 RT mutants in free or complexed form are also available. Several HIV related databases are maintained at Los Alamos National Laboratory (www.hiv.lanl.gov.) [15]. NIST (National Institute of Standards and Technology) runs the" HIV Structural

¹Institute of Theoretical Chemistry, University of Vienna, Währinger Straße 17, A-1090 Vienna, Austria

²Department of Common and Graduate Studies, Sirindhorn International Institute of Technology (SIIT), Thammasat University, Thammasat Rangsit, Pathumthani 12121, Thailand

³Department of Chemistry, Faculty of Science, Ubonratchathani University, Ubonratchathani 34190, Thailand

^{*}Address correspondence to this author at the Institute of Theoretical Chemistry, University of Vienna, Währinger Straße 17, A-1090 Vienna, Austria; Fax: +43-1-4277 52771; Tel: ++43 1 4277 9527; E-mail: Anton.Bever@univie.ac.at

Table 1. Sequences of Two Variants of HIV-1 RT (S1 and S2)

1	PISPIETVPV KLKPGMDGPK VKQWPLTEEK IKALVEICTE MEKEGKISKI GPENPYNTPV	60
1	PISPIETVPV KLKPGMDGPK VKQWPLTEEK IKALVEICTE MEKEGKISKI GPENPYNTPV	60
61	FAIKKKDSTK WRKLVDFREL NKRTQDFWEV QLGIPHPAGL KKKKSVTVLD VGDAYFSVPL	120
61	FAIKKKDSTK WRKLVDFREL NKRTQDFWEV QLGIPHPAGL KKKKSVTVLD VGDAYFSVPL	120
121	DEDFRKYTAF TIPSINNETP GIRYQYNVLP QGWKGSPAIF QSSMTKILEP F ${f R}$ KQNPDIVI	180
121	DEDFRKYTAF TIPSINNETP GIRYQYNVLP QGWKGSPAIF QSSMTKILEP F $\underline{\mathbf{K}}$ KQNPDIVI	180
181	YQYMDDLYVG SDLEIGQHRT KIEELRQHLL RWGLTTPDKK HQKEPPFLWM GYELHPDKWT	240
181	YQYMDDLYVG SDLEIGQHRT KIEELRQHLL RWGLTTPDKK HQKEPPFLWM GYELHPDKWT	240
241	VQPIVLPEKD SWTVNDIQKL VGKLNWASQI YPGIKVRQLC KLLRGTKALT EVIPLTEEAE	300
241	VQPIVLPEKD SWTVNDIQKL VGKLNWASQI YPGIKVRQLC KLLRGTKALT EVIPLTEEAE	300
301	LELAENREIL KEPVHGVYYD PSKDLIAEIQ KQGQGQWTYQ IYQEPFKNLK TGKYARMRGA	360
301	LELAENREIL KEPVHGVYYD PSKDLIAEIQ KQGQGQWTYQ IYQEPFKNLK TGKYARMRGA	360
361	HTNDVKQLTE AVQKITTESI VIWGKTPKFK LPIQKETWET WWTEYWQATW IPEWEFVNTP	420
361	HTNDVKQLTE AVQKITTESI VIWGKTPKFK LPIQKETWET WWTEYWQATW IPEWEFVNTP	420
421	PLVKLWYQLE KEPIVGAETF YVDGAANRET KLGKAGYVTN ${f R}$ GRQKVV ${f T}$ LT ${f D}$ TTNQKTELQ	480
421	PLVKLWYQLE KEPIVGAETF YVDGAANRET KLGKAGYVTN K GRQKVV P LT N TTNQKTELQ	480
481	AIYLALQDSG LEVNIVTDSQ YALGIIQAQP D Q SESELVNQ IIEQLIKKEK VYLAWVPAHK	540
481	AIYLALQDSG LEVNIVTDSQ YALGIIQAQP D K SESELVNQ IIEQLIKKEK VYLAWVPAHK	540
541	GIGGNEQVDK LVSAGIRK <u>V</u> L	560
541	GIGGNEQVDK LVSAGIRK I L	560
	1 61 61 121 121 181 181 241 241 301 361 361 421 481 481 541	1 PISPIETVPV KLKPGMDGPK VKQWPLTEEK IKALVEICTE MEKEGKISKI GPENPYNTPV 61 FAIKKKDSTK WRKLVDFREL NKRTQDFWEV QLGIPHPAGL KKKKSVTVLD VGDAYFSVPL 61 FAIKKKDSTK WRKLVDFREL NKRTQDFWEV QLGIPHPAGL KKKKSVTVLD VGDAYFSVPL 121 DEDFRKYTAF TIPSINNETP GIRYQYNVLP QGWKGSPAIF QSSMTKILEP FRKQNPDIVI 121 DEDFRKYTAF TIPSINNETP GIRYQYNVLP QGWKGSPAIF QSSMTKILEP FKQNPDIVI 181 YQYMDDLYVG SDLEIGQHRT KIEELRQHLL RWGLTTPDKK HQKEPPFLWM GYELHPDKWT 181 YQYMDDLYVG SDLEIGQHRT KIEELRQHLL RWGLTTPDKK HQKEPPFLWM GYELHPDKWT 181 VQPIVLPEKD SWTVNDIQKL VGKLNWASQI YPGIKVRQLC KLLRGTKALT EVIPLTEEAE 180 VQPIVLPEKD SWTVNDIQKL VGKLNWASQI YPGIKVRQLC KLLRGTKALT EVIPLTEEAE 180 LELAENREIL KEPVHGVYYD PSKDLIAEIQ KQGQGQWTYQ IYQEPFKNLK TGKYARMRGA 181 LELAENREIL KEPVHGVYYD PSKDLIAEIQ KQGQGQWTYQ IYQEPFKNLK TGKYARMRGA 182 HTNDVKQLTE AVQKITTESI VIWGKTPKFK LPIQKETWET WWTEYWQATW IPEWEFVNTP 183 HTNDVKQLTE AVQKITTESI VIWGKTPKFK LPIQKETWET WWTEYWQATW IPEWEFVNTP 184 PLVKLWYQLE KEPIVGAETF YVDGAANRET KLGKAGYVTN RGRQKVVTLT DTTNQKTELQ 185 AIYLALQDSG LEVNIVTDSQ YALGIIQAQP DQSESELVNQ IIEQLIKKEK VYLAWVPAHK 186 AIYLALQDSG LEVNIVTDSQ YALGIIQAQP DRSESELVNQ IIEQLIKKEK VYLAWVPAHK 187 GIGGNEQVDK LVSAGIRKYL

Database" which has some additional information not included in PDB (http://xpdb.nist.gov/hivsdb/hivsdb.html) [16].

Two variants of slightly different protein sequences have been used throughout these studies, denoted here as S1 and S2. Both sequences are given in Table $\bf 1$.

In this table the differences between the two variants are shown. There is one difference in the Palm domain, whereas the others are located in the RNase H domain [17, 18].

A summary of all structures currently available in PDB is given in Table $\bf 2$.

Table 2. HIV-1 Reverse Transcriptase X-ray structures in the Protein Data Bank. Resolution (Res) in Å

	PDB Code	Ligand	Res	Year	Ref.	Model	Mutation	
1	1RTI	НЕРТ	3.00	1995	[19]	S1 560	-	
2	1RT1	MKC-422 Emivirine	2.55	1996	[20]	S1 560	-	
3	1RT2	TNK-651	2.55	1996	[20]	S1 560	-	
4	1JLA	TNK-651	2.50	2001	[21]	S1 560	Y181C	
5	1S1V	TNK-651	2.60	2004	[22]	S1 560	L100I	
6	1C1B	GCA-186	2.50	1999	[23]	S1 560	-	
7	1C1C	TNK-6123	2.50	1999	[23]	S1 560	-	
8	IJLQ	739W94	3.00	2001	[24]	S1 560	-	
9	1HNV	8-C1 TIBO (R86183)	3.00	1995	[25]	S2 558	C280S	
10	1UWB	8-Cl TIBO (R86183)	3.20	1996	[26]	S2 558	C280S	Y181C
11	1TVR	9-Cl TIBO (R82913)	3.00	1996	[26]	S2 558	C280S	
12	1REV	9-Cl TIBO (R82913)	2.60	1995	[27]	S1 560	-	

(Table 2)contd

				T	T	1	(Tab	le 2)contd				
	PDB Code	Ligand	Res	Year	Ref.	Model	Mutation					
13	3HVT	Nevirapine (Viramune)	2.90	1994	[28,29]	S2 556	-					
14	1VRT	Nevirapine (Viramune)	2.20	1995	[19]	S1 560	-					
15	1FKP	Nevirapine (Viramune)	2.90	2000	[30]	S1 543	K103N					
16	1JLB	Nevirapine (Viramune)	3.00	2001	[21]	S1 560	Y181C					
17	1JLF	Nevirapine (Viramune)	2.60	2001	[21]	S1 560	Y188C					
18	1LWC	Nevirapine (Viramune)	2.62	2002	[31]	S1 560	M184V					
19	1LW0	Nevirapine (Viramune)	2.80	2002	[31]	S1 560	T215Y					
20	1LWE	Nevirapine (Viramune)	2.81	2002	[31]	S1 560	M41L	T215Y				
21	1LWF	Nevirapine (Viramune)	2.80	2002	[31]	S1 560	M41L	D67N				
	K70R	M184V										
	T215Y											
22	1S1U	Nevirapine (Viramune)	3.00	2004	[21]	S1 560	L100I					
23	1S1X	Nevirapine (Viramune)	2.80	2004	[22]	S1 560	V108I					
24	1RTH	1051U91	2.20	1995	[19]	S1 560	-					
25	1RT3	1051U91	3.00	1998	[32]	S1 555	D67N	K70R				
	T115F	K219Q										
26	1LW2 1051U91	3.00	2002	[31]	S1 560	T215Y						
27	1VRU	2,6-Cl2 a-APA (R90385)	2.40	1995	[19]	S1 560	-					
28	1HPZ	2,6-Cl2 a-APA (R90385)	3.00	2000	[33]	S2 560	K103N	C280S				
29	1HNI	2,6-Br2 a-APA (R95845)	2.80	1995	[34]	S2 558	C280S					
30	1BQM	HBY097	3.10	1998	[35]	S2 556	C280S					
31	1BQN	HBY097	3.30	1998	[35]	S2 558	Y188L	C280S				
	E248Q	E546Q										
32	1HQU	HBY097	2.70	2000	[33]	S2 560	K103N	C280S				
33	1KLM	BHAP U-90152	2.65	1997	[27]	S1 560	-					
34	1RT5	UC-10	2.90	1998	[27]	S1 560	-					
35	1RT6	UC-38	2.80	1998	[27]	S1 560	-					
36	1RT7	UC-84	3.00	1998	[27]	S1 560	-					
37	1RT4	UC-781	2.90	1998	[27]	S1 560	-					
38	1JLG	UC-781	2.60	2001	[21]	S1 560	Y188C					
39	1S1T	UC-781	2.40	2004	[22]	S1 560	L100I					
40	1S1W	UC-781	2.70	2004	[22]	S1 560	V106A					
41	1COT	BM+21.1326	2.70	1999	[37]	S1 560	-					
42	1COU	BM+50.0934	2.52	1999	[37]	S1 560	-					
43	1DTT	PETT-2 (PETT130A94)	3.00	2000	[38]	S1 560	-					
44	1JLC	PETT-2	3.00	2001	[21]	S1 560	Y181C					
45	1DTQ	PETT-1 (PETT131A94)	2.80	2000	[38]	S1 560	-					
46	1EET	MSC204	2.73	2000	[39]	S2 557	E478Q					
47	1IKY	MSC194	3.00	2001	[40]	S2 560	K103N	E478Q				

(Table 2)contd.....

(Table	le 2)contd												
	PDB Code	Ligand	Res	Year	Ref.	Model	Mutation						
48	1IKX	PNU142721	2.80	2001	[40]	S2 560	K103N	E478Q					
49	1FK9	DMP-266 (Efavirenz)	2.50	2000	[30]	S1 543	-						
50	1IKW	DMP-266 (Efavirenz)	3.00	2001	[40]	S2 560	E478Q						
51	1FKO	DMP-266 (Efavirenz)	2.90	2000	[30]	S1 543	K103N						
52	1IKV	DMP-266 (Efavirenz)	3.00	2001	[40]	S2 560	K103N	E478Q					
53	1JKH	DMP-266 (Efavirenz)	2.50	2001	[21]	S1 560	Y181C						
54	1EP4	S-1153	2.50	2000	[41]	S1 560	-						
55	1S6P	R100943	2.90	2005	[42]	S2 560	C280S						
56	1S9G	R120394	2.80	2005	[42}	S2 560	C280S						
57	1S9E	R129385	2.60	2005	[42]	S2 560	C280S						
58	1S6Q	R147681	3.00	2005	[42]	S2 560	C280S						
59	2BAN	R157208	2.95	2005	[43]	S2 560	C280S						
60	1SV5	R165335	2.90	2004	[42]	S2 560	C280S	K103N					
61	2B5J	R165481	2.90	2005	[43]	S2 560	C280S						
62	1SUQ	R185545	3.00	2005	[42]	S2 560	C280S						
63	2BE2	R221239	2.43	2005	[43]	S2 560	C280S						
64	1TKT	GW426318	2.60	2004	[44]	S1 560	-						
65	1TKZ	GW429576	2.81	2004	[44]	S1 560	-						
66	1TKX	GW490745	2.85	2004	[44]	S1 560	-						
67	1TL3	GW450557	2.80	2004	[44]	S1 560	_						
68	1TL1	GW451211	2.90	2004	[44]	S1 560	-						
69	1TV6	CP-94	2.80	2004	[45]	S2 560	-						
70	2B6A	THR-50	2.65	2005	[46]	S2 560	C280S						
71	1HAR	-	2.20	1994	[47]	NA 216	N-Term						
72	1HMV	-	3.20	1994	[48]	S2 560	-						
73	1RTJ	-	2.35	1995	[49]	S1 560	-						
74	1DLO	-	2.70	1996	[50]	S2 556	C280S						
75	1HQE	-	2.70	2000	[51]	S2 560	K103N	C280S					
76	1JLE	-	2.80	2001	[21]	S1 560	Y188C						
77	1QE1	-	2.85	1999	[51]	S2 558	C280S	M184I					
78	2HMI	DNA/FAB	2.80	1998	[52,53]	S2 558	C280S						
79	1C9R	DNA/FAB	3.50	1999	[51]	S2 556	C280S	M184I					
80	1J5O	DNA/FAB	3.50	2002	[51]	S2 558	C280S	M184I					
81	1T05	DNA/Fab	3.00	2004	[54]	S2 558	C280S	Q258C					
82	1T03	DNA/Fab	3.10	2004	[54]	S2 558	C280S	Q258C					
83	1N6Q	DNA/Fab	3.00	2002	[55]	S2 558	C280S	Q258C					
84	1N5Y	DNA/Fab	3.10	2002	[55]	S2 558	C280S	Q258C					
85	1RTD	DNA/dNTP	3.20	1998	[56]	S1 553	Q258C	R461K					
	T468P	E478Q											

(Table 2)contd....

	PDB Code	Ligand	Res	Year	Ref.	Model	Mutation	
	Q512E							
86	1HVU	RNA	4.75	1998	[57]	S2 554	-	
87	1HYS	RNA/DNA	3.00	2001	[58]	S2 553	C280S	

HIV-1 RT is a heterodimer and contains two chains with identical amino acid sequences but of different lengths. The first chain (p66), has a molecular weight of 66kDa and consists of 560 amino acids. The second chain (p51) is built up from 440 residues and has a molecular weight of 51kDa. It lacks the RNase H domain at the C-terminus. Both subunits contain a polymerase domain composed of four subdomains, called fingers, palm, thumb and connection. p66 and p51 are expressed by the same gene and their sequences are therefore identical (p51 is processed by proteolytic cleavage of p66). Nevertheless, the polymerase subdomains are arranged in different way, p66 forming a large-active site pocket (with the catalytic triad Asp110, Asp185 and Asp186) and p51 with a closed and therefore inactive structure. The complete structure of HIV-1 RT (p66 and p51) is shown in Fig. 1.

1.4. Structure of the HIV-1 RT NNRTI Binding Site

NRTIs and NtRTIs bind to the active center, whereas the binding pocket for NNRTIs is about 10Å away from the catalytic site. This cavity is located between two β -sheets (β 4, β 7 and β 8 of the fingers domain - amino acids 73-77, 128-134, 141-147, and $\beta 9$, $\beta 10$ and $\beta 11$ – amino acids 178-183, 186-191, 214-217 and 219-222 of the palm domain of p66 by. Additionally, the β5-β6 loop (Pro97, Leu100, Lys101, Lys103), β6 (Ser105, Val106, Val108), the hairpins β9-β10 (Val179, Tyr181, Tyr188, Gly190, Asp192), and \(\beta12-\beta13\) (Glu224, Phe227, Trp229, Leu234, Pro236), and two amino acids β15 (Tyr318, Tyr319) of the thumb domain [18]. Two amino acids from p51 (Thr135,

Glu138) are also involved in the inhibitor. The binding pocket is mainly hydrophobic, with some aromatic amino acids (Tyr181, Tyr188, Phe227, Trp229, Tyr232) but includes a few hydrophilic residues (Lys101, Lys103, Ser105, Asp192, Glu224) and backbone atoms, which are able to form hydrogen bonds. These structural features of the binding site are highly important for the association of inhibitors. The entrance to the cavity is formed by residues Leu100, Lys103, Val179, Ser191 and Glu138 from p51. Examples for the interaction of various inhibitors with amino acids in the NNRTI binding pocket are outlined in Table 3.

The table indicates residues which have distances less than 4Å to the related inhibitor in the X-ray crystal structure. The importance of Leu100, Lys101 (β6 of palm domain), Tyr181, Tyr188 (β9 of palm domain), Trp229 (β12 of palm domain) and Tyr318 (β15 of thumb domain) can be easily deduced. These amino acids are in close contact with almost every inhibitor. Superpositions of four structures of NNRTIs, HEPT, TIBO, nevirapine and efavirenz, attached to the WT HIV-1 RT binding pocket are presented in Fig. 2.

1.5. Structural Requirements for NNRTIs

A butterfly-like shape with two hydrophobic, mostly aromatic wings, was postulated as pharmacophor for NNRTI. However, for second generation inhibitors this molecular shape gets less stringent, but there is still a similarity in shape and charge distribution. Not surprisingly, also hydrogen bonding

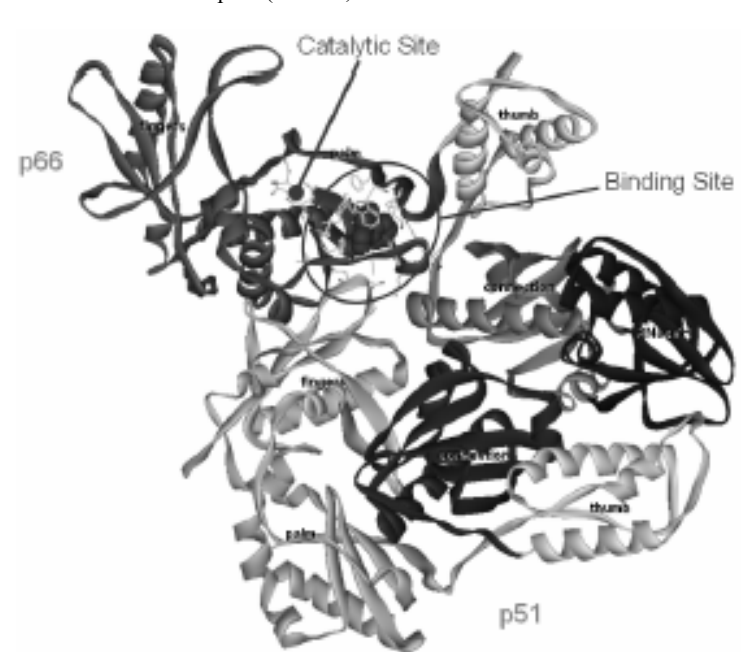


Fig. (1). Structure of HIV-1 RT.

Table 3. Amino acid residues in contact with NNIs within the distance of 4Å

	Ē	Ę	Ę	<u></u>	Ü	ō	3	HU	109/8	ITYR	IREV	TAHE	LYRT	PKP	11.8	1.	RTH	Ę	LVRU	1	4 3		2	2	DH.	3	Ę	RTB	Ē	RT4	2	6	₫	Ë	¥	5	I EET	ΠΚΥ	Σ	PKO	IIK &	<u> </u>	HKY	LIKH	1874	280N	2831	2862
Mutebool				ı					ı					2	. 1				1		2			J	2						J				3							2	. 2	. 1				
Pro93										Х	Х			Х			×	×	τ				х								х	х					х	Х	Х							х		х
LeuIDD	×	х	х	х	Х	х	Х	х	Х	×	Х	Х	Х	Х	×	×	×	X	()	€.	х	х	х	х	х	х	х	х	х	х	х	х	Х	х	Х	х	Х	х	х	х	х	х	Х	х	х	х	Х	×
LysiDi	×	х	х	х	Х	х	Х	х	Х	×	Х	Х	Х	Х	×	×	×	X	()	€.	х	х	х	х	х	х	х	х	х	х	х	х	Х	х	Х	х	Х	х	х	х	х	х	Х	х	х	х	Х	×
Lys102							Х																			Х													Х						х			
Lys100	×	х	х	х	х	х	Х	Х	Х	Х	Х	Х		Х)	C		х			х	х	х	х	Х	х	х	х	Х	х	х	Х	Х	Х	Х	Х	Х	Х		Х	Х	х	Х	: ж
Lys104																										Х																						
Ser103			х																																													
V41106	Х	х	х	х	х	Х	Х		Х	Х	Х	Х	Х	Х	×	X	×	×	()	€.				х	Х	Х	х	Х	Х	х	Х	х	х	х	х	Х	Х	Х	Х	Х	х	Х	Х	Х	х		Х	ж
TB/107																						х																										
Val108																																															Х	×
Val179	×	х	х				Х	Х			Х		Х	Х	×	×	×	X	()	€.	х	х	х	х			х	х	х	х	х	х		х	Х	х	Х	Х	Х	Х	х	Х	Х	Х	х	х	Х	×
He13D								Х			Х														Х								х															
Tyviði															-		-	-		-	-																										-	ж
Tyriaa	ж				Х				Х	х	Х	Х	Х					(X								х	х	х			х			х	Х	х	Х	х	х									×
A9135			х				Х									×								х					Х				х										Х					
Gly190		х	х	х	Х	х	Х				Х	Х	Х	Х	×	X)	€.	х	х	х	х	х		х		х	х	х	х	Х					х	х	х	х	х	х	х	х	х	Х	ж
Glu224																										Х																						
Pro223	х	х	х	х		Х																	х			х											Х	Х							х			
Pro226																										х																						
Pbe 227	х	х	х	х	Х	х		х	Х		Х	х	х	х	×	X	×	X	τ				х		х	х		х	х	х	х			х		х	Х	х	х	х	х	х	х	х	х			×
Leu 223																																															Х	
Trp229			х						Х																							х	х						Х									×
Leu234			х									Х			×														х	х																		ж
H:5233	х							Х		х	Х		Х				×	-		•		х	х		х	х						х											Х				Х	×
Pro236			х									Х					×	-		•				х			х				х												х					ж
Туузта	×	х	х	х	Х	х	Х	х	Х	х	Х			х	×	×	×	(X	()	€.	х	х	х	х	х	х	х	х	х	х	х	х	Х	х	Х	х	Х	х	х	х	х	х	х	х	х	х	Х	ж
Tyvalo												Х																																				
Asa136*																	×																															
Cini 39,							х									×		×	()	€.	х	х						х		х	х		х	х	х	х	х	х						х		х		

^amutation code:

- 1 Tyr181Cys
- 2 Lys103Asn
- 3 Tyr188Cys
- 4 Asp67Asn, Lys70Arg, Thr215Phe, Lys219Gln

plays an important role for the association specificity and affinity of the various inhibitors.

2. MOLECULAR SIMULATIONS OF THE INTERACTION BETWEEN NNRTIS AND HIV-1 RT

X-ray crystal structures of proteins and protein ligand complexes deliver valuable information about the geometries of such aggregates, which can be used for further investigations like structure based drug design. There are some restrictions for this method so far, as the structural information is bound to solid state, and, moreover, no information about the dynamics of the systems can be given - in contrast to another very important method for elucidation of biomolecular geometries, the nuclear magnetic resonance spectroscopy (NMR). Because of the size of the protein no NMR experiments can be performed on RT up to now. Moreover, for in silico screening of large numbers of compounds and for the target based design of new drugs the geometries of enzyme-inhibitor complexes have to be determined. The specific association of drugs to a well-defined binding site at the receptor is controlled by the energetics of the system, the sum of local interactions between the molecular

surface of the ligand and the complementary surface of the receptor. Various methods of molecular docking, using proper force fields provide some possibilities to obtain possible orientations of the ligands in the receptor pocket. Molecular dynamics (MD) and Monte-Carlo simulations (MC) are used to get some insight into the dynamical behaviour of protein-ligand interactions taking into account the surrounding, the solvent shell or even membrane structures. Depending on the quality of the molecular calculations the latter methods need large computer resources. Nevertheless, both methods are nowadays routinely used and are widely applied in newer strategies for calculations of protein-ligand complexes. Particularly, combinations of molecular docking, energy minimization and molecular dynamics simulations are promising tools for drug design investigations.

2.1. Molecular Docking to HIV-1 RT

Many newly synthesized NNRTI candidates were tested by docking to targets obtained form crystal structures. Deng *et al.* [59] visualized hypothetical complex models for a series of alkenyldiarylmethane derivatives using the molecular docking

bamino acid residues of p51

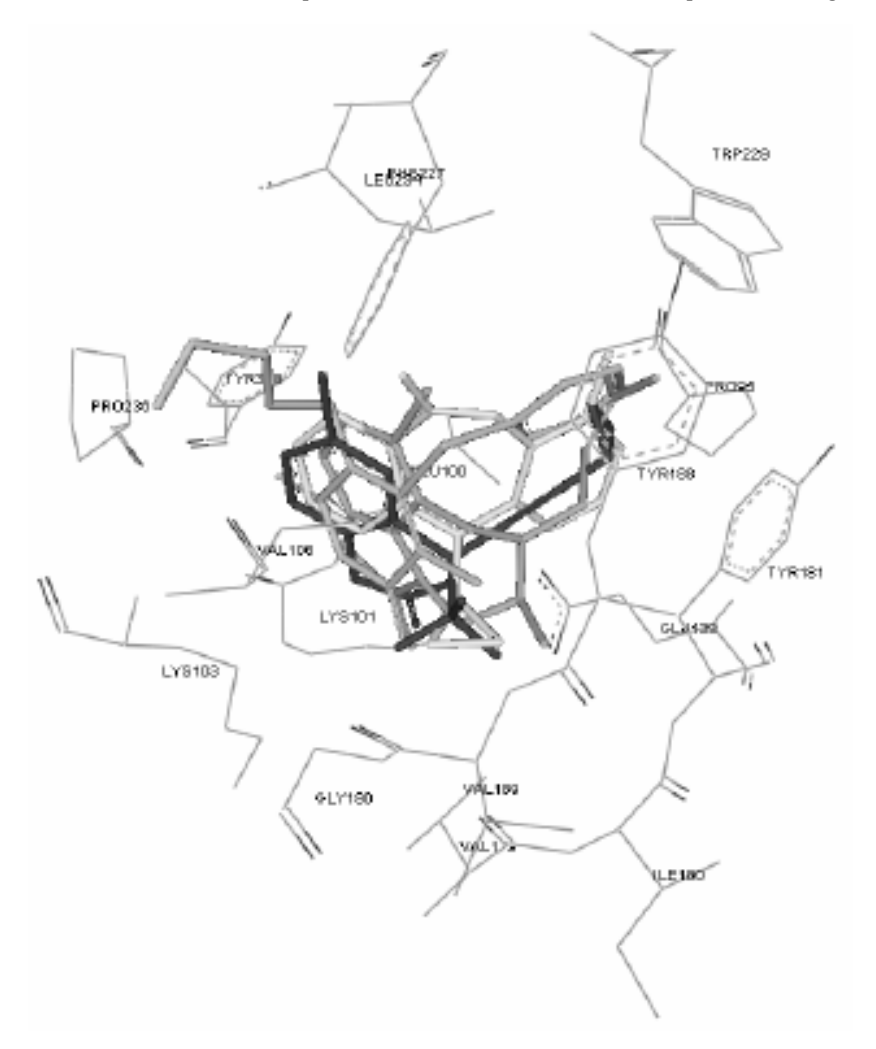


Fig. (2). Superimposition of four X-ray structures of NNRTIS, HEPT (1RTI, shown in gray), TIBO (1HNV, shown in dark gray), nevirapine (1VRT, shown in light gray) and efavirenz (1FK9, shown in black), bound to the WT HIV-1 RT binding pocket.

method GLIDE (Schrödinger Inc.). Other examples of very recent applications of various docking procedures are: Heeres et al. [60], De Martino et al. [61], Heemateenejad et al. [62], Medina-Franco et al. [63], Zhou et al. [64], Sciabola et al. [65], Ranise et al. [66].

Extensive docking studies using AutoDock [67] have been performed by Ragno et al. [68] to test the applicability of this method for reproducing the geometries obtained from X-ray crystallography and, to undertake cross-docking experiments on the wild-type and mutant type enzyme's structures.

Docking studies have been used in combination with other methods. Chen et al. [69] combined molecular docking, MD simulations and Support Vector Machine (SVM) based methods to predict new compounds of the class of 3',4'-di-O-(S)camphanyl-(+)-cis-Khellactone analogs.

QSAR investigations together with docking simulations were applied on indoyl aryl solfunes [70], Barrecca et al. [71] combined flexible docking with QSAR studies. Evidently, data base screening uses also different docking methods. A recent expample is the work of Sangma et al. [72]. A fast and robust computational method for predicting NNRTIs activities by correlating molecular docking energies and biologically activities was proposed by de Jonge [73].

2.2. MD and MC Simulations of HIV-1 RT and of Complexes with NNRTIs

Generally, the applicability of MD simulations increases with the development of more sophisticated methods and related computer power. Free energy calculations and the structural information from MD simulations contribute to the advanced computer-assisted techniques in drug discovery and drug design [74]. However, not too many investigations have been published on RT MD simulations. The reason for this fact is, that HIV-1 RT is a very large system. When hydrogen atoms are added, The 556 and 427 amino acid residues in p66 and p51 subunits of RT alone (1DLO), consists of 16,000 atoms after adding hydrogen atoms to the X-rax crystal structure data. If an eight Å truncated octahedral box with water molecules is added, the system will carry almost 40,000 water molecules. MD of this enzyme requires a huge computer resource with respect to calculation time and mass storage.

A MD simulation of HIV-1 RT indicating subdomain rearrangements was reported by Madrid et al. [75], another simulation showed increasing flexibility upon DNA binding [76].

Gardozo et al. [77] reported a MD simulation of the p66 subunit of RT with nevirapine. Tyrosine 181 showed a remarkable interaction with the inhibitor during this MD simulation. Monte Carlo methods (MC) in combination with a linear response approach [78], adaptive chemical Monte Carlo/molecular dynamics (CMC/MD), and Poisson-Boltzmann/solvent accessibility (PB/SA) [79,80] were used to determine the relative binding free energies to HIV-1 RT of TIBO and efavirenz series with rather encouraging results. Wang et al. [81] proposed that molecular docking combined with MD simulations (500 ps) followed by Molecular Mechanics Poisson-Boltzmann/surface area (MM-PBSA) analysis is an attractive approach for modeling the protein a priori. In this work, the obtained binding mode of efavirenz to HIV-1 RT in aqueous solvent was in reasonable agreement with X-ray crystallographic experiments. The binding and unbinding processes of another NNRTI, α-APA, have been investigated using two nanoseconds molecular dynamics and steered molecular dynamics simulations (SMD). The bound α-APA was pulled out from the binding pocket of HIV-1 RT by employing an artificial harmonic potential on α-APA [82]. Only p66 subunit (without RNase H subdomain) was involved in this simulation with water. The results show that the polar group of α-APA plays key roles in inhibition and binding.

In June 2005, the 2.5 nanoseconds MD simulations of complete solvated HIV-1 RT systems (approximately 142,000 atoms) were handled by Zhou et al. [83] on the Terascale Computing System at the Pittsburgh Supercomputing Center. The flexibility of wild type and mutant RT complexed to nevirapine was studied and the free energy of binding was calculated using Molecular Mechanics Poisson-Boltzmann Surface Area (MM-PBSA). Nevirapine interacts stronger with wild-type RT than with mutant RT as a consequence of the diminished van der Waals interactions between the inhibitor and the amino acid around the binding pocket. Their simulations point out that the flexibility of RT depends on the volume of the binding pocket occupied by the inhibitor. Weinzinger et al. [80] applied successfully MD analyses to obtain prediction models, correlating the binding energies for efavirenz and a series of its derivatives, benzoxazinones, with experimental inhibitory activities. Moreover, the importance of the hydrogen bonding interaction of this class of inhibitors with Lys101 and electrostatic interactions with Lys101 and His235 was demonstrated. Similar considerations based on MC simulations have been undertaken by Rizzo et al. [84]. The molecular basis of resilience in NNRTI to the effect of a mutation was the topic of a paper of Rodriguez-Barrios et al. [85].

3. STRUCTURE-ACTIVITY RELATIONSHIP STUDIES OF HIV-1 INHIBITORS

The second important concept for the design of new drugs is the use of Quantitative Structure-Activity Relationship analyses (QSAR). From correlations between quantitative biological effects with molecular descriptors prediction models can be created, which are taken furthermore to design new drugs. The general problems for the use of such methods are first of all the accuracy of the biological data, which might be created by different research groups, and the selection and determination of proper molecular descriptors, which should be able to describe the most important molecular features for the particular activity. There are two steps to generate a QSAR model; calculation of molecular descriptors, and statistical generation

of the QSAR model. Therefore, QSAR approaches can be divided into two main types: classical or two dimensional QSAR (2D-QSAR) and three dimensional QSAR analysis (3D-QSAR), classified by the descriptors used. 2D-QSAR descriptors do not utilize 3D information concerning the ligand and their geometries, dependent on the specific conformation and the orientation of the molecules. This approach requires no structural alignment of molecules in the data set. In contrast, the 3D structure and also the structure dependent molecular fields of ligands are strongly involved in descriptor calculations used to derive a 3D-QSAR model. In the case of such conformation dependent descriptors the alignment of the molecules is a challenging task, which could lead in worst case to misguided statements.

Many drugs have been developed in the last years for anti HIV-1 activities on the several viral targets, some of them are already on the market or in clinical proof [6,7]. Virtual screening based on structure based design lead to numerous candidates for new drugs and this process will continue, due to the necessity to overcome increasing drug resistance caused by mutations. QSAR studies concentrate mainly on distinct groups of compounds as the development of a general model is not possible even for identical targets, due to changes of the mechanism of action of different types of inhibitors. An attempt to discriminate between active and non-active compounds against HIV-1 has been done recently [86]. Various inhibition mechanisms on different targets with totally 2720 active and inactive compounds have been included in the study using a probabilistic network. Although the prediction power of the obtained model is good (around 85% of the external prediction series are correct), a quantitative comparison with biological data will be not possible.

3.1. 2D-QSAR Analyses of HIV-1 RT Inhibition

Numerous classes of structural different classes of compounds have been identified as NNRTIs, which bind to an allosteric, non-substratebinding site of the enzyme. Three NNRTIs have been licensed for clinical use: nevirapine (Viramune), efavirenz (Sustiva, Stocrin) and delavirdine (Rescriptor). Many QSAR studies were performed to identify important structural features responsible for the inhibition. Based on multiple linear regression analysis, Garg et al. [87-91] developed 2D-QSAR models for several classes of compounds, HEPT, TIBO, nevirapine, pyridinone, BHAP, TSAO and α-APA derivatives using physicochemical parameters of the inhibitors calculated by the C-QSAR program. On the basis of the obtained QSAR models, the most of models reported for NNRTIs involve significant hydrophobic terms. However, the absence of any hydrophobic interactions for α-APA derivatives was found. Electrotopological state atom (ETST) indices were used as new molecular descriptors to set up QSAR models of a series of TIBO, HEPT and arylsulfonylbenzonitrile derivatives [92-94]. The predictive and informative models were obtained proposing that the atom or fragmental level descriptors are more useful to interpret drug-receptor interactions in these analogues.

Hannongbua *et al.* [95, 96] successfully set up 2D-QSAR models to NNRTIs in the class of HEPT and TIBO derivatives by using various structural descriptors obtained from quantum chemical calculations. The obtained models indicate the importance of electronic and molecular properties contributing to HIV-1 inhibitory potency. The performance and

applicability of semi-empirical and ab-initio calculations with respect to the OSAR analysis of HEPT analogues were performed. The models derived by AM1 and ab initio HF/3-21G seem to be the most suitable in terms of both statistical significance and predictive ability. Based on structural parameters, the obtained models indicate that molecular polarizability and atomic charges of the hydrogen atom of the thymine group and the amino group nitrogen play an important role for the affinity of HEPT derivatives. However, the QSAR models of nevirapine compounds using similar structural parameters could not be satisfactorily derived for both WT and Tyr181Cys HIV-1 RT inhibitory activities. Probably, the descriptors used are insufficient to explain the variance of the data set. In an attempt to improve the quality of the QSAR model, additional descriptors such as connectivity and topological indices were used and an artificial neural network was applied [97]. The obtained non-linear QSAR models show satisfactory relationships between the molecular descriptors used and the inhibition of WT and mutant HIV-1 RT. In addition to nevirapine derivatives, neural networks were applied to other classes of potent NNRTIs such as HEPT and TIBO analogues [86, 98-104]. The main factors contributing to the binding affinity of the inhibitors have been determined. Hologram QSAR (HQSAR) [HQSAR, Tripos, Inc., (1997), St. Louis, MO], is a 2D-QSAR approach, which describes the molecular structural compositions in terms of substructural fragments and is independent on the alignments of the considered molecules. This method was applied successfully on three different inhibitors in the class of TIBO, HEPT and nevirapine compounds. The results are able to explain the relationship between molecular holograms constructed from counting the molecular fragments and the HIV-1 inhibition potency of that class of substances. HQSAR model provides hints about how molecular fragments may be important descriptors to biological activity. The molecule is color coded to reflect the individual

atomic contributions to activity. The colors at the red end of the spectrum (red, red orange and orange) reflect unfavorable contributions, while colors at the green end (yellow, green, blue and green) reflect favorable contributions. Atoms with intermediate contributions are colored white. As x-ray crystallographic structures of HIV-1 RT complexes with inhibitors are available, the amino acid residues surrounding TIBO, HEPT and dipyridodiazepinone in the binding pocket were merged into inhibitors to get a better understanding the interactions between the inhibitor-enzyme. The HQSAR results can be helpful to indicate the similarity interactions of these three molecular diverse analogues of HIV-1 RT inhibitors, as depicted in Fig. 3. The obtained results indicated that HQSAR method can be a useful tool in providing important structural features of HIV-1 RT inhibitors [105].

Medina –Franco *et al.* [63] developed QSAR models for highly potent NNRTIs of pyridinone derivatives by using the k nearest neighbor (kNN) variable selection approach. The models with high internal and external accuracy were generated. The best models were successfully used to search for the promising new NNRTI leads from the National Cancer institute database.

3.2. 3D-QSAR Analyses of HIV-1 RT Inhibition

3D-QSAR analyses take into account the steric interactions between ligand and protein and, moreover, they include geometry-dependent molecular properties like electrostatic field, or hydrogen bond donor or acceptor abilities. Comparative molecular field analysis (CoMFA) is one of the most powerful 3D-QSAR techniques providing further insight into the relationships between three-dimensional properties of molecules and the biological activity of these compounds and functions of inhibitor [106]. Additional to CoMFA approach, comparative molecular similarity indices analysis (CoMSIA) [107], which takes additionally into account more molecular 3D

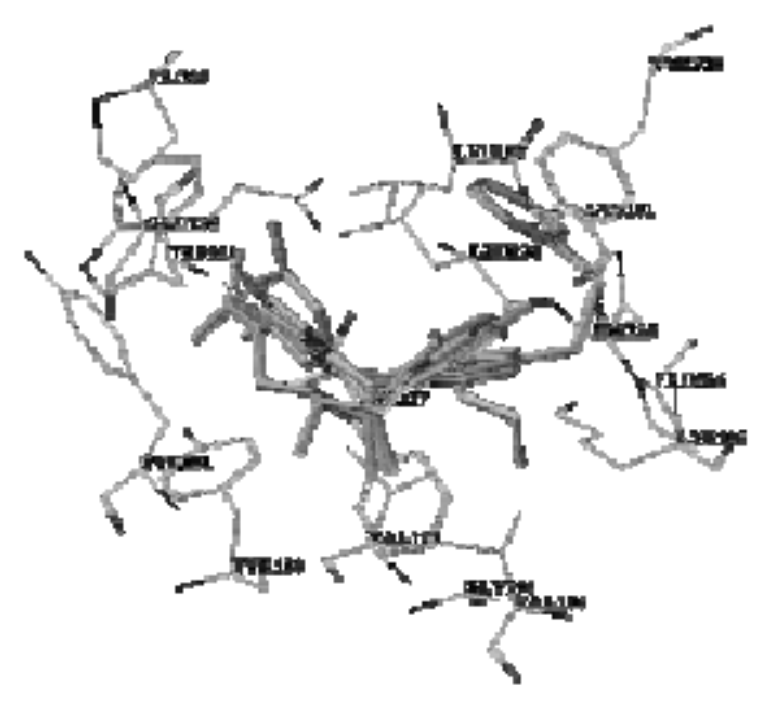
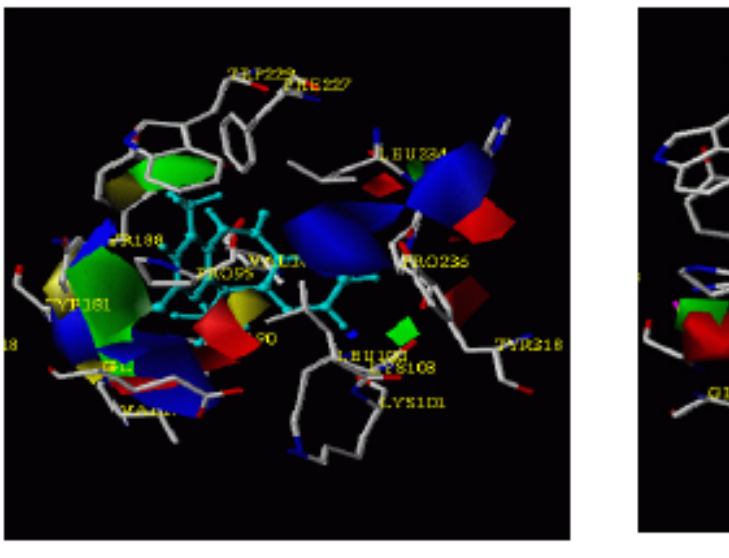


Fig. (3). Superimposition of TIBO, HEPT, nevirapine derivatives, color coded by the best obtained HQSAR model, in the binding pocket of HIV-1 RT. [105]

properties, like hydrogen bond donor and acceptor properties, is most commonly used in drug design process to find the common features that are important for binding of the drugs to the biologically relevant receptor [108]. A review about the application of various 3D-QSAR techniques in the design of anti-HIV drugs has been given by Debnath [109]. The crucial step of using many 3D-QSAR techniques, particularly CoMFA or CoMSIA lies on the alignment rule. To derive reliable models for good predictive power, many attempts have to be performed to search for the best molecular alignment, which generally corresponds to the orientation of the ligand at the receptor site. Based on the atom-by-atom alignment of all molecules on the template molecule, selected from the highest active compounds of each data set, predictive QSAR models were successfully obtained in establishing the relationship between the fields around molecules with their biological activities through contour maps.

CoMFA prediction models of HEPT together with TIBO derivatives were considered by Hannongbua et al. [96, 110, 111], showing the importance of both steric and electrostatic fields for the interaction of these class of inhibitors with the RT. Corresponding to the WT and Tyr181Cys HIV-1 RT inhibitions, CoMFA and CoMSIA models for nevirapine derivatives were derived with satisfactory predictive ability and statistical significance [112, 113]. The contour maps highlight different characteristic for different types of wild-type and mutant type HIV-1 RT, as presented in Figs. 4 and 5. The interpretation of CoMFA and CoMSIA models reinforces each other and shows good accordance with the inhibitor-receptor complex derived from the experimental data. Consequently, the obtained results not only lead to a better understanding of important enzymeligand interaction and also provide helpful information in identifying structural requirements for the design of new and more potent compounds active against HIV-1 RT. A 3D-QSAR



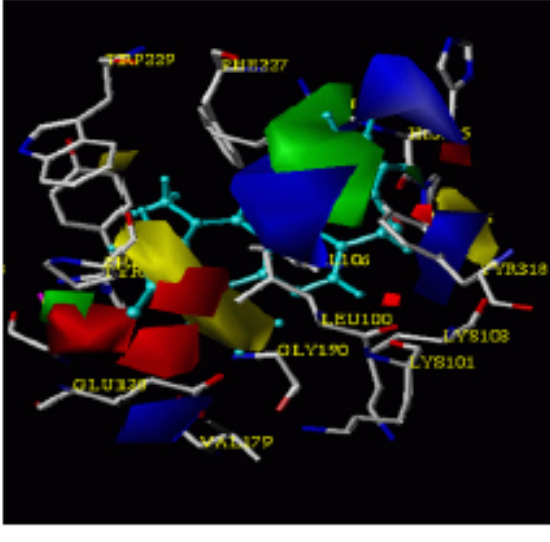
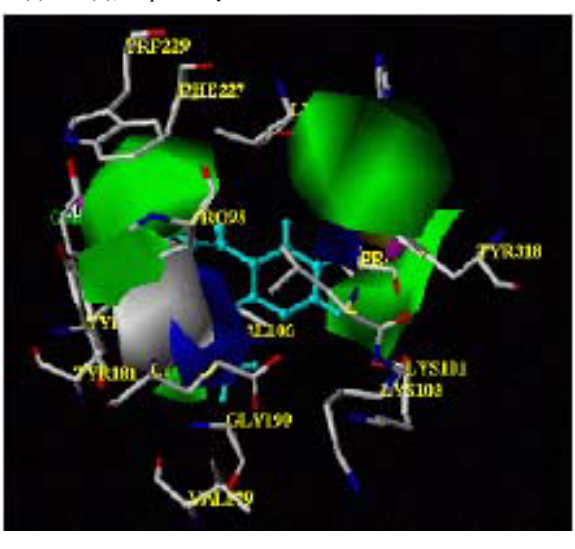


Fig. (4). CoMFA steric and electrostatic STDEV*COEFF contour plots of nevirapine derivatives based on WT and Tyr181Cys HIV-1 RT inhibitions, as shown in (a) and (b), respectively.



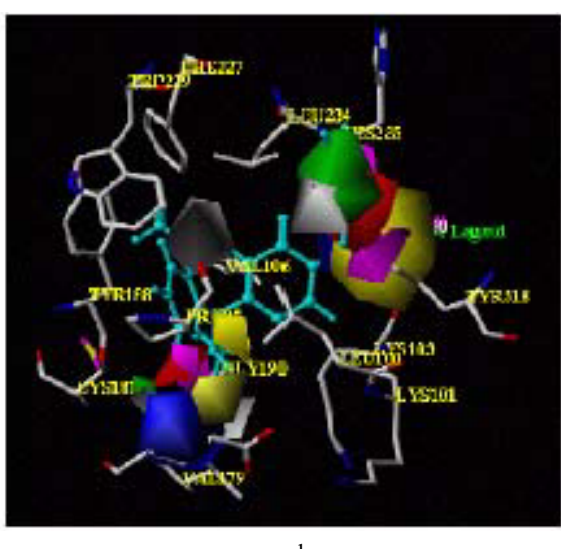


Fig. (5). CoMSIA steric, electrostatic and hydrophobic STDEV*COEFF contour plots of nevirapine derivatives based on WT and Tyr181Cys HIV-1 RT inhibitions, as shown in (a) and (b), respectively.

study based on the program HINT was also given by Gussio et al. [114].

CoMFA and CoMSIA models of efavirenz analogues were successfully developed by Pungpo et al. [115, 116] in order to explain the relationship between structural properties and HIV-

1 inhibition. The information obtained from all models apparently reveals differentiating structural requirements between WT and Lys103Asp HIV-1 RT inhibitory activities of these inhibitors. The obtained results can be integrated to provide a fundamental guideline to design and predict the new

Table 4. QSAR studies on NNRTIs

NNRTIs	QSAR methods	References
НЕРТ	MLR-QSAR	[87, 93, 95]
	NN-QSAR	[86, 98, 99, 100, 101, 102, 103]
	HQSAR	[105]
	CoMFA	[110, 111, 117]
	CoMFA CoMSIA	[119]
	4D-QSAR	[124]
TIBO	MLR-QSAR	[87, 91, 92, 96]
	NN-QSAR	[86, 104]
	HQSAR	[105]
	CoMFA	[71, 96]
	CoMFA CoMSIA	[119, 121]
Nevirapine	MLR-QSAR	[87]
	NN-QSAR	[86, 97]
	HQSAR	[105]
	CoMFA	[112]
	CoMFA CoMSIA	[113]
	3D-QSAR (HINT)	[114]
	4D-QSAR	[123]
Efavirenz	CoMFA CoMSIA	[115, 116]
Pyridinone	MLR-QSAR	[87]
	NN-QSAR	[63, 86]
	CoMFA CoMSIA	[122]
Arylsulfonylbenzonitrile	MLR-QSAR	[94]
	3D-QSAR	[126]
Benzenonitrile	3D-QSAR	[65]
Indolarylsulfone	3D-QSAR	[70]
Phthalimide	CoMFA CoMSIA	[120]
Quinolone	3D-QSAR	[118]
Alpha-APA	MLR-QSAR	[87]
ВНАР	MLR-QSAR	[87]
TSAO	MLR-QSAR	[87, 90]
	NN-QSAR	[86]
3-[N-(phtalimido)-5-ethyl-6-methylpyridin-2(1H)-one	MLR-QSAR	[88]
acyclouridine	MLR-QSAR	[89]

compounds with enhancing HIV-1 RT inhibitory activities active against WT and Lys103Asp HIV-1 RT. Barreca et al. [71] applied CoMFA and molecular docking to a set of TIBO derivatives endowed with reverse transcriptase inhibitory activity. The predictive model was obtained from the combination of steric and electrostatic fields and molecular lipophilicity potential.

Kireev et al. [117] applied a special method, creating 3D descriptors for a statistical analysis to a large dataset of HEPT derivatives. A similar approach was reported by Filipponi et al. [118], who applied a combination between Volsurf and GRID on a set of quinolone derivatives. 2D-descriptors were created from 3D-grid map without superimposition of the molecules.

Chen et al. [119] applied molecular docking, CoMFA and CoMSIA approaches to binding mode investigation of NNRTI in the class of HEPT and TIBO derivatives. Partial and global 3D-QSAR models were built, based on the molecular alignment of conformations obtained from molecular docking procedures. The results demonstrate that the obtained model show better prediction ability compared to 2D-QSAR models. A CoMFA and CoMSIA based investigation on a small number of phthalimides was reported by Samee et al. [120]. 3D-QSAR approaches have been applied to derive prediction models of the NNRTI classes of TIBO, pyridinone and indolylarylsulfones (IASs) derivatives [70,121,122]. With the combination of ligand-(GRIND) and structure-based (GLUE/GRIND) 3D-QSAR approaches, the 3D-OSAR models of (aryl-)bridged 2-aminobenzenonitriles analogues were developed and compared [65]. It can be seen from the study that the GRIND approach allows the deviation of the valid 3D-QSAR models even in the absence of proper X-ray information. A summary of QSAR studies on selected groups of compounds is given in Table 4.

As the detailed information concerning intermolecular interaction in three dimension is still required to encode, several 3D-QSAR approaches have been developed. Ligand 4D-QSAR analysis, developed by Hopfinger et al. [123], based on the grid cell occupancy as descriptors, incorporates conformational and alignment freedom. A series of nevirapine derivatives was selected as training set. The general findings from the applications are that the grid cell occupancy descriptors associated with the constant chemical structure of an analog series can be significant in the 3D-QSAR models and there is a large data reduction. Recently, the 4D-QSAR method coupled with PLS analysis and uninformative variable elimination was applied to investigate the antiviral activity of a series of HEPT compounds [124]. The results show that the method properly indicates the mode of interaction revealed by X-ray studies and is used to generate highly predictive QSAR models. COMBINE analysis [125] were successfully applied to derive the 3D-OSAR models which are able to take into account for the variance in biological activities of highly potent NNRTIs in a class of arylsulfonylbenzonitrile derivatives. The obtained models are fruitfully used to provide chemometrical identification of mutations in HIV-1 RT conferring resistance or enhanced sensitivity to the inhibitors [126].

Evidently, QSAR approaches are widely and successfully applied to derive the key structural features of several classes of HIV-1 RT NNRTIs. The common structural requirements obtained provide an insight into a structure-activity relationship of ligands to their binding sites, leading to valuable guideline in predicting new and more potent

inhibitors. Although, the major limitation of QSAR application is the use within congeneric series of compounds, OSAR methodology has been proven as an attractive and efficient tool in medicinal and pharmaceutical chemistry.

4. PERSPECTIVES

As the combat against HIV is of high importance, many experimental data and also theoretical considerations are available. The complete understanding of the mechanisms of the action of the multifunctional enzyme RT is as important as the cognition of the detailed inhibition mechanism for the development of new drugs. Moreover, the influence of mutations in the drug interacting disease proteins on the inhibition reaction has to be investigated carefully. The structures of RT and of the complexes with inhibitors or DNA obtained from X-ray crystallographic analyses deliver information about the structural changes induced by association of NNRTI to an allosteric binding pocket, and, moreover, structural requirements for new inhibitors can be recognized, particularly with respect to mutations. The increasing number of X-ray structures and the application of various theoretical methods will lead to an easier access to new, maybe more efficient drugs. The rapid determination of sequences of viral proteins from various patients and the subsequent prediction of the structure of mutants of RT could facilitate the application of tailored drugs for a faster more efficient offense against AIDS. Increasing possibilities of computer technology, together with the development of new, and more sophisticated simulation methods will allow to determine the dynamical behavior of biomolecular assemblies, in particular the motions of domains involved in the enzyme's activity and the inhibition reaction. Finally, the combination of various theoretical methods will lead to faster and more accurate algorithms to perform QSAR studies and in silico screening. E.g. weaknesses like the molecular alignment in 3D-QSAR or the ambiguities in docking procedures in virtual screening can be avoided by such combinatorial procedures. All these encouraging options will enable the medicinal chemists to support medicinal research much stronger and more efficient in very next future.

ACKNOWLEDGEMENTS

The authors would like to thank Prof. Hannongbua for her encouragement to write this mini-review. Financial support from the Thailand Research Fund (MRG4880001) is gratefully acknowledged, as well as technical assistance of Mrs. E. Liedl and Ms. M. Ziehengraser. Special thanks to Ms. P. Saparpakorn for her excellent assistance in preparing the manuscript.

REFERENCES

- Frankel, A.D.; Young, J.A.T. Ann. Rev. Biochem., 1998, 67, 1-25. [1] [2]
- Coffin, J.M. (Ed.); Retroviruses, Cold Spring Harbor Laboratory Press, Cold Spring Harbor, New York, 1997.
- De Clercq, E. J. Clin. Vir., 2001, 22, 73-89.
- De Clercq, E. Biochim. Biophys. Acta, 2002, 1587, 258-275. [4]
- De Clercq, E. Nature Rev. Drug Discov., 2002, 11, 13-25.
- De Clercq, E. Chem. Biodiver., 2004, 1, 44-64.
- De Clercq, E. J. Med. Chem., 2005, 48, 1297-1313.
- De Clercq, E. Front. Med. Chem., 2004, 1, 543-579.
- Tarrago-Litvak, L.; Andreola, M.L.; Fournier, M.; Nevinsky, G.A.; Parissi, V.; De Soultrait, V.R.; Litvak, S. Curr. Pharm. Des., 2002, 8,

- Campiani, G.; Ramunno, A.; Maga, G.; Nacci, V.; Fattorusso, C.; Catalanotti, B.; Morelli, E.; Novellino, E. Curr. Pharm. Des., 2002, 8, [10]
- De Clercq, E. Antiv. Res., 1998, 153-179.
- Clavel, F.; Hance, A.J. New Engl. J. Med., 2004, 350, 1023-1035. Cao, Z.W.; Han, L.Y.; Zheng, C.J.; Ji, Z.L.; Chen, X.; Lin, H.H.; Chen, Y.Z. Drug Discover., 2005, 10, 521-529. [12] [13]
- Shafer, R.W.; Kantor, R.; Gonzales, M.J. AIDS Rev., 2000, 2, 168-177.
- Berman, H.M.; Westbrook, J.; Feng, Z.; Gilliland, G.; Bhat, T.N.; Weissig, H.; Shindyalov, I.N.; Bourne, P.E. *Nucleic Acids Research*, **2000**, *28*, 235-242. [15]
- [16] Leitner, T.; Foley, B.; Hahn, B.; Marx, P.; McCutchan, F.; Mellors, J.; Wolinsky, S.; Korber, B. (Eds) Published by Theoretical Biology and Biophysics Group, Los Alamos National Laboratory, NM, LA-UR 06-0680.
- Vondrasek, J.; Wlodawer, A. Proteins, 2002, 49, 29 31.
- Lawtrakul, L.; Beyer, A.; Hannongbua, S.; Wolschann, P. Monatsh. Chem., 2004, 135, 1033-1046. [18]
- [19] Beyer, A.; Lawtrakul, L.; Hannongbua, S.; Wolschann, P. Monatsh. Chem., 2004, 135, 1047-1059.
- Ren, J.; Esnouf, R.; Garman, E.; Somers, D.; Ross, C.; Kirby, I.; Keeling, J.; Darby, G.; Jones, Y.; Stuart, D.; Stammers, D. Nat. Struct. Biol., **1995**, *2*, 293-302.
- Hopkins, A.L.; Ren, J.; Esnouf, R.M.; Willcox, B.E.; Jones, E.Y.; Ross, T211 C.; Miyasaka, T.; Walker, R.T.; Tanaka, H.; Stammers, D.K.; Stuart, D.I. J. Med. Chem., 1996, 39, 1589-6000.
- Ren, J.; Nichols, C.; Bird, L.; Chamberlain, P.; Weaver, K.; Short, S.; Stuart, D.I.; Stammers, D.K. *J. Mol. Biol.*, **2001**, *312*, 795-805. [22]
- Ren, J.; Nichols, C.; Chamberlain, P.; Weaver, K.; Short, S.; Stammers, [23] D.K. J. Mol. Biol., 2004, 336, 569-578.
- Hopkins, A.L; Ren, J.; Tanaka, H.; Baba, M.; Okamato, M.; Stuart, D. I.; Stammers, D.K. *J. Med. Chem.*, **1999**, *42*, 4500-4505. [24]
- Chan, J.H.; Hong, J.S.; Hunter, R.N.III.; Orr, G.F.; Cowan, J.R.; Sherman, D.B.; Sparks, S.M.; Reitter, B.E.; Andrews, C.W.III.; Hazen, [25] R.J.St.; Clair, M.; Boone, L.R.; Ferris, R.G.; Creech, K.L.; Roberts, G.B.; Short, S.A.; Weaver, K.; Ott, R.J.; Ren, J.; Hopkins, A.; Stuart, D.I.; Stammers, D.K. *J. Med. Chem.*, **2001**, *44*, 1866-1882. Ding, J.; Das, K.; Moereels, H.; Koymans, L.; Andries, K.; Janssen,
- [26] P.A.J.; Hughes, S.H.; Arnold, E. Nat. Struct. Biol., 1995, 2, 407-415.
- Das, K.; Ding, J.; Hsiou, Y.; Clark Jr., A.D.; Moereels, H., Koymans; L.; Andries, K.; Pauwels, R.; Janssen, P.A.J.; Boyer, P.L.; Clark, P.; Smith Jr., R.H.; Kroeger Smith, M.B.; Michejda, C.J.; Hughes, S.H.; Arnold, E. [27] J. Mol. Biol., 1996, 264, 1085-1100.
- [28]
- Stant, D. Structure, 1995, 15, 915-926.
 Smerdon, D.J.; Jaeger, J.; Eang, J.; Kohlstaedt, L.A.; Chirino, A.J.; Friedman, J.M.; rice, P.A.; Steitz, T.A. Proc. Natl. Acad. Sci. USA, 1994, [29] 91, 3911-3915.
- Wang, J.; Smerdon, S.J.; Jaeger, J.; Kohlstaedt, L.A.; Rice, P.A.; Friedman, J.M.; Steitz, T.A. *Proc. Natl. Acad. Sci. USA*, **1994**, *91*, 7242-[30]
- Ren, J.; Milton, J.; Weaver, K.L.; Short, S.A.; Stuart, D.I.; Stammers, [31]
- D.K. Structure, **2000**, *8*, 1089-1094. Chamberlain, P.; Ren, J.; Nichols, C.; Douglas, L.; Lennerstrand, J.; Larder, B.A.; Stuart, D.I.; Stammers, D.K. *J. Virol.*, **2002**, *76*, 10015-[32]
- Hsiou, Y., Ding, J.; Das, K.; Clark Jr., A.D.; Boyer, P. L.; Lewi, P.; Janssen, P.A.J.; Kleim, J.P.; Roesner, M.; Hughes, S.H.; Amold, E. *J. Mol. Biol.*, **2001**, *309*, 437-445. [33]
- Ding, J.; Das, K.; Tantillo, C.; Zhang, W.; Clark, A.D.Jr.; Jessen, S.; Lu, [34] X.; Hsiou, Y.; Jacobo-Molina, A.; Andries, K.; Pauwels, R.; Moereels, H.; Koymans, L.; Janssen, P.A.J.; Smith Jr., R.H.; Kroeger Koepke, M.; Michejda, C.J.; Hughes, S.H.; Arnold, E. Structure, 1995, 3, 365-379.
- Hsiou, Y.; Das, K.; Ding, J.; Clark, A.D. Jr.; Kleim, J.P.; Roesner, M.; Winkler, I.; Riess, G.; Hughes, S.H.; Amold, E. J. Mol. Biol., 1998, [35] 284. 313-323.
- Esnouf, R.M.; Ren, J.; Hopkins, A.L.; Ross, C.K.; Jones, E.Y.; [36] Stammers, D.K.; Stuart, D.I. Proc. Natl. Acad. Sci. USA, 1997, 94, 3984-
- [37] Ren, J.; Esnouf, R.M.; Hopkins, A.L.; Warren, J.; Balzarini, J.; Stuart,
- D.I.; Stammers, D.K. *Biochemistry*, **1998**, *37*, 14394-14403. Ren, J.; Esnouf, R.M.; Hopkins, A.L.; Stuart, D.I.; Stammers, D.K. *J. Med. Chem.*, **1999**, *42*, 3845-3851. T381
- [39] Ren, J.; Diprose, J.; Warren, J.; Esnouf, R.M.; Bird, L.E.; Ikemizu, S.; Slater, M.; Milton, J.; Balzarini, J.; Stuart, D.I.; Stammers, D.K. *J. Biol. Chem.*, **2000**, *275*, 5633-5639.
- Hogberg, M., Sahlberg, C.; Engelhardt, P.; Noreen, R.; Kangasmetsa, J.; Johansson, N.G.; Oberg, B.; Vrang, L.; Zhang, H.; Sahlberg, B.L.; [40] Unge, T.; Lovgren, S.; Fridborg, K.; Backbro, K. J. Med. Chem., 1999, 42 4150-4160
- [41] Lindberg, J.; Sigurosson, S.; Lowgren, S.; Andersson, H.O.; Sahlberg, C.; Noreen, R.; Fridborg, K.; Zhang, H.; Unge, T. Eur. J. Biochem., 2002, 269, 1670-1677.
- Ren, J.; Nichols, C.; Bird, L.E.; Fujiwara, T.; Sugimoto, H.; Stuart, D.I.; Stammers, D.K. *J. Biol. Chem.*, **2000**, *275*, 14316-14320. [42]

- Das, K., Clark, A.D. Jr.; Lewi, P.; Heeres, J.; De Jonge, M.; Koymans, L.; Vinkers, H.; Daeyaert, F.; Ludovici, D.W.; Kukla, M.J.; De Corte, B.; Kavash, R.W.; Ho, C.Y.; Ye, H.; Lichtenstein, M.; Andries, K.; Pauwles, [43] R.; De Bethune, M.P.; Boyer, P.L.; Clark, P.; Hughes, S.H.; Janssen, P.A.; Arnold, E. *J. Med. Chem.*, **2004**, *47*, 2550-2560. Himmel, D.M.; Das, K.; Clark, A.D.Jr.; Hughes, S.H.; Benjahad, A.;
- [44] Oumouch, S.; Guillemont, J.; Coupa, S.; Poncelet, A.; Csoka, I.; Meyer, C.; Andries, K.; Nguyen, C.H.; Grierson, D.S.; Arnold, E. J. Med. Chem., 2005, 48, 7582-7591.
- Hopkins, A.L.; Ren, J.; Milton, J.; Hazen, R.J.; Chan, J.H.; Stuart, D.I.; Stammers, D.K. *J. Med. Chem.*, **2004**, *47*, 5912-5922. [45]
- [46] Pata, J.D.; Stirtan, W.G.; Goldstein, S.W.; Steitz, T.A. Proc. Nat. Acad. Sci. USA, 2004, 101, 10548-10553.
- Morningstar, M.L.; Roth, T.; Smith, M.K.; Zajac, M.; Watson, K.; [47] Buckheit, R.W.; Das, K.; Zhang, W.; Arnold, E.; Michejda, C.J. to be published.
- Unge, T.; Knight, S.; Bhikhabhai, R.; Lovgren, S.; Dauter, Z.; Wilson, K.; Strandberg, B. Structure, 1994, 2, 953-961. Rodgers, D.W.; Gamblin, S.J.; Harris, B.A.; Ray, S.; Culp, J.S.; Hellmig,
- [49] B.; Woolf, D.J.; Debouck, C.; Harrison, S.C. Proc. Natl. Acad. Sci. USA, 1995, 92, 1222-1226.
- [50] Esnouf, R.; Ren, J.; Ross, C.; Jones, Y.; Stammers, D.; Stuart, D. Nat. Struct. Biol., 1995, 2, 303-308. Hsiou, Y.; Ding, J.; Das, K.; Clark Jr., A.D.; Hughes, S.H.; Arnold, E.
- [51] Structure, 1996, 4, 853-860.
- [52] Sarafianos, S.G.; Das, K.; Clark, A.D.Jr.; Ding, J.; Boyer, P.L.; Hughes,
- S.H.; Arnold, E. *Proc. Natl. Acad. Sci. USA*, **1999**, *96*, 10027-10032. Jacobo-Molina, A.; Ding, J.; Nanni, R.G.; Clark, A.D.; Lu, X.; Tantillo, C.; Williams, R.L.; Kamer, G.; Ferris, A.L.; Clark, P.; Hizi, A.; Hughes, [53] S.H.; Arnold, E. *Proc. Natl. Acad. Sci. USA*, **1993**, *90*, 6320-6324. Ding, J.; Das, K.; Hsiou, Y.; Sarafianos, S.G.; Clark, A.D.; Jacobo-
- [54] Molina, A.; Tantillo, C.; Hughes, S.H.; Arnold, E. J. Mol. Biol., 1998, 284, 1095-1111.
- Tuske, S.; Sarafianos, S.G.; Clark Jr., A.D.; Ding, J.; Naeger, L.K.; White, K.L.; Miller, M.D.; Gibbs, C.S.; Boyer, P.L.; Clark, P.; Wang, G.;
- White, R.L., Miller, M.D., Globs, C.S., Boyer, F.L., Clark, F., Wang, G., Gaffney, B.L.; Jones, R.A.; Jerina, D.M.; Hughes, S.H.; Arnold, E. *Nat. Struct. Mol. Biol.*, **2004**, *11*, 469-474.
 Sarafianos, S.G.; Clark Jr., A.D.; Das, K.; Tuske, S.; Birktoft, J.J.; Ilankumaran, I.; Ramesha, A.R.; Sayer, J.M.; Jerina, D.M.; Boyer, P.L.; Hughes, S.H.; Arnold, E. EMBO J., 2002, 21, 6614-6624.
- Huang, H.; Chopra, R.; Verdine, G.L.; Harrison, S.C. Science, 1998, 282, 1669-1675. [57]
- Jaeger, J.; Restle, T.; Steitz, T.A. EMBO J., 1998, 17, 4535-4542
- Sarafianos, S.G.; Das, K.; Tantillo, C.; Clark, A.D. Jr.; Ding, J.; Whitcomb, J.M.; Boyer, P.L.; Hughes, S.H.; Arnold, E. *EMBO J.*, **2001**, [59] 20. 1449-1461.
- [60] Deng, B.L.; Cullen, M.D.; Zhou, Z.G.; Hartmann, T.L.; Buckheit, R.W.; Pannecouque, C.; De Clercq, E.; Fanwick, P.E.; Cushman, M. Bioorg. Med. Chem., 2006, 14, 2366-2374. Heeres, J.; de Jonge, M.R.; Koymans, L.M.H.; Daeyaert, F.F.D.; Vinkers,
- [61] M.; Van Aken, K.J.A.; Arnold, E.; Das, K.; Kilonda, A.; Hoornaert, G.J.; Compernolle, F.; Cegla, M.; Azzam, R.A.; Andries, K.; de Bethune, M.P.; Azijn, H.; Pauwels, R.; Lewi, P.J.; Janssen, P.A.J. J. Med. Chem., 2005, 48, 1910-1918.
- De Martino, G.; La Regina, G.; Di Pasquali, A.; Ragno, R.; Bergamini, [62] A.; Ciaprini, C.; Sinistro, A.; Maga; G.; Crespan, E.; Artico, M.; Silvestri, R. J. Med. Chem., 2005, 48, 4378-4388.
- Hemmateenejad, B.; Tabaei, S.M.H.; Namvaran, F. J. Mol. Struct. THEOCHEM, 2005, 732, 39-45. [63]
- Medina-Franco, J.L.; Golbraikh, A.; Oloff, S.; Castillo, R.; Tropsha, A. J. [64] Comput. Aid. Mol. Des., 2005, 19, 229-242.
- Zhou, Zhigang; Madrid, M; Madura, J.D. Proteins: Struct. Funct. Gen.,
- **2002**, 49, 529-542. Sciabola, S.; Carosati, E.; Baroni, M.; Mannhold, R. J. Med. Chem., **2005**, 48, 3756 -3767. [66] Ranise, A.; Spallarossa, A.; Cesarini, S.; Bondavalli, F.; Schenone, S.;
- Bruno, O.; Menozzi, G.; Fossa, P.; Mosti, L.; La Colla, M.; Sanna, G.; Murreddu, M.; Collu, G.; Busonera, B.; Marongiu, M.E.; Pani, A.; La Colla, P.; Loddo, R. J. Med. Chem., 2005, 48, 3858-3873.
- Goodsell, D.S.; Morris, G.M.; Olson, A.J. J. Mol. Recognit., 1996, 9, 1-[68]
- [69] Ragno, R.; Frasca, S.; Manetti, F.; Brizzi, A.; Massa, S. J. Med. Chem., 2005, 48. 200-212. [70] Chen, H.F.; Fan, B.T.; Zhao, C.Y.; Xie, L.; Zhao, C.H.; Zhou, T.; Lee,
- K.H.; Allaway, G. J. Comput. Aid. Mol. Des., 2005, 19, 243-258. [71] Ragno, R.; Artico, M.; De Martino, G.; La Regina, G.; Coluccia, A.; Di
- Pasquali, A.; Silvestri, R. J. Med. Chem., 2005, 48, 213-223. Barreca, M.L.; Carotti, A.; Carrieri, A.; Chimirri, A.; Monforte, A.M.; [72] Calace, M.P.; Rao, A. Bioorg. Med. Chem., 1999, 7, 2283-2292.
- Sangma, C.; Chuakheaw, D.; Jongkon, N.; Saenbandit, K.; Nunrium, P.; Uthayopas, P.; Hannongbua, S. Comb. Chem. High Throughput Screen., 2005, 8, 417- 429.
- De Jonge, M.R.; Koymans, L.M.H.; Vinkers, H.M.; Daeyaert, F.F.D.; [74] Heeres, J.; Lewi, P.J.; Janssen, P.A.J. J. Med. Chem., 2005, 48, 2176-2183.

- Hansson, T.; Oostenbrink, C.; Van Gunsteren, W.F. Curr. Opin. in Struct. Biol., 2002, 12, 190-196.
 Madrid, M.; Lukin, J.A.; Madura, J.D.; Ding, J.; Arnold, E. Proteins: [75]
- [76] Struct. Func. Gen., 2001, 45, 176-182.
- Madrid; M.; Jacobi-Molina, A.; Ding, J.; Arnold, E. Proteins: Struct. Func. Gen., 1999, 35, 332-337. [77]
- [78] Cardozo, M.G.; Tong, L.; Jones, P.J. J. Mol. Graphics, 1993, 11, 272-
- Smith Jr., R.H.; Jorgensen, W.L.; Tirado-Rives, J.; Lamb, M.L.; Janssen, P.A.J.; Michejda, C.J.; Smith, M.B.K. J. Med. Chem., 1998, 41, 5272-[79] 5286.
- [80] Eriksson, M.A.L.; Pitera, J.; Kollman, P.A. J. Med. Chem., 1999, 42, 868-881.
- Weinzinger, P.; Hannongbua, S.; Wolschann, P. J. Enz. Inhib. Med. T811 Chem., 2005, 20, 129-134.
- Wang, J.M.; Morin, P.; Wang, W.; Kollman, P.A. J. Med. Chem., 2001, [82] *123*, 5221-5230.
- Shen, L.L.; Shen, J.H.; Luo, X.M.; Cheng, F.; Xu, Y.C.; Chen, K.X; Arnold, E.; Ding, J.P.; Jiang, H.L. *Biophys. J.*, **2003**, *84*, 3547-3563. Zhou, Z.; Madrid, M.; Evanseck, J.D.; Madura, J.D. *J. Am. Chem. Soc.*, [83]
- [84] **2005**, 127, 17253-17260.
- Rizzo, R.C.; Udier-Blagovic, M.; Wang, De-Ping; Watkins, E.K.; Kroeger Smith, M.B.; Smith, R.H.; Tirado-Rives, J.; Jorgensen, W.L. *J. Med. Chem.*, **2002**, *45*, 2970-2987. [85]
- [86] Rodriguez-Barrios, F.; Balzarini, J.; Gago, F. J. Am. Chem. Soc., 2005, *127*, 7570-7578.
- Vilar, S.; Santana, L.; Uriarte, E. J. Med. Chem., 2006, 49, 1118-1124.
- Garg, R.; Gupta, S.P.; Gao, H.; Babu, M.S.; Debnath, A.K.; Hansch, C. *Chem. Rev.*, **1999**, *99*, 3525-3601. [88]
- Garg, R.; Gupta, S.P. J. Enzyme Inh., 1997, 12, 1-12. [89]
- Garg, R.; Kurup, A.; Gupta, S.P. Quant. Struc.-Act. Relat., 1997, 16, [90] 20- 24.
- Garg, R.; Gupta, S.P. J. Enzyme Inh., 1997, 11, 171-181.
- Gupta, S.P.; Garg, R. J. Enzyme Inh., 1996, 11, 23-32. [92]
- [93] Huuskonen, J. J. Chem. Inf. Mod., 2001, 41, 425-429.
- [94] Gayen, S.; Debnath, B.; Samanta, S.; Jha, T. Bioor. Med. Chem., 2004, 12. 1493-1503.
- Roy, K.; Leonard, J.T. Bioorg. Med. Chem., 2004, 12, 745-754.
- [96] Hannongbua, S.; Lawtrakul, L.; Limtrakul, J. J. Compt. Aided Mol. Des., **1996,** 10, 145-152.
- Hannongbua, S.; Pungpo, P.; Limtrakul, J.; Wolschann, P. J. Comput. Aid. Mol. Des., 1999, 13, 563-577. [97]
- Prasithichokekul, S.; Pungpo, P.; Hannongbua, S.; Ecker, G.; Wolschann, P. Proceedings of the 5th annual national symposium on
- computational science and engineering. Academic, Bangkok, 2001, 351. Jalali-Heravi, M.; Parastar, F., J. Chem. Inf. Comput. Sci., 2000, 40, 147-[99]
- [100] Bazoui, H.; Zahouily, M.; Boulaajai, S.; Sebti, S.; Zakarya, D. SAR and
- QSAR Env. Res., 2002, 13, 567-577.
 Douali, L.; Villemin, D.; Cherqaoui, D. J. Chem. Inf. Mod., 2003, 43, [101] 1200-1207.

- [102]
- Mager, P.P. Curr. Med. Chem., 2003, 10, 1643-1659. Douali, L.; Villemin, D.; Cherqaoui, D. Curr. Pharm. Des., 2003, 9, [103] 1817-1826.
- [104] Chiu, T.L.; So, S.S. J. Chem. Inf. Mod., 2004, 44, 154-160.
- Douali, L.; Villemin, D.; Cherqaoui, D. Int. J. Mol. Sci., 2004, 5, 48-55. Pungpo, P.; Hannongbua, S.; Wolschann, P. Curr. Med. Chem., 2003, [105]
- [106] 10. 1661-1677
- Cramer, R.D.; Patterson, D.E.; Bunce, J.D. J. Am. Chem. Soc., 1988, [107] 110, 5959-5967.
- F1081 Klebe, G.; Abraham, U. J. Comput. Aid. Mol. Des., 1999, 13, 1-10.
- Klebe, G.; Abraham, U.; Mietzner, T. J. Med. Chem., 1994, 37, 4130-[109]
- Debnath, A.K. Curr. Pharm. Des., 2005, 11, 3091-3110.
- Hannongbua, S.; Lawtrakul, L.; Sotriffer, C.A.; Rode, B.M. Struct.-Act. Relat., 1996, 15, 389-394. [111]
- [112] Hannongbua, S.; Nivesanond, K.; Lawtrakul, L.; Pungpo, P.; Wolschann, P. J. Chem. Inf. Mod., 2001, 41, 848-855. Pungpo, P.; Hannongbua, S. J. Mol. Graph. Mod., 2000, 18, 581-590.
- [113] Pungpo, P.; Wolschann, P.; Hannongbua, S. The proceeding of the [114] International Conference on Bioinformatics 2002, North - South
- Networking, Le Royal Meridien, Bangkok, Thailand. Gussio, R.; Pattabiraman, N.; Zaharevitz, D.W.; Kellogg, G.E.; Toplo, I.A.; Rice, W.G.; Schaeffer, C.A.; Erickson, J.W.; Burt, S.K. *J. Med. Chem.*, **1996**, *39*, 1645-1650. [115]
- [116] Pungpo, P.; Wolschann, P.; Hannongbua, S. The proceeding of the 15th European symposium on quantitative structure-activity
- relationships and molecular modelling, Euro QSAR 2004, Istanbul, TURKEY Pungpo, P.; Saparpakorn, P.; Wolschann, P.; Hannongbua. S. 3rd [117]
- International Symposium Computational Methods in Toxicology and Pharmacology Integrating Internet Resources, 2005, Shanghai, China Kireev, D.B.; Chretien, J.R.; Grierson, D.S.; Monneret, C. J. Med. [118]
- Chem., 1997, 40, 4257-4264.
 Filipponi, E.; Cruciani, G.; Tabarrini, O.; Cecchetti, V.; Fravolini, A. J.
- [119] Comput. Aid. Mol. Des., 2001, 15, 203-217. Chen, H.F.; Yao, X.J.; Li, Q.; Yuan, S.G.; Panaye, A.; Doucet, J.P.; Fan,
- [120] B.T. SAR and OSAR in Environ. Res., 2003, 14, 455-474.
- Γ1211 Samee, W.; Ungwitayatorn, J.; Matayatsuk, C.; Pimthon, J. ScienceAsia, 2004, 30, 81-84.
- Γ1221 Zhou, Z.; Madura, J.D. J. Chem. Inf. Mod., 2004, 44, 2167-2178
- Medina-Franco, J.L.; Rodriguez-Morales, S.; Juarez-Gordiano, C.; Hernandez-Campos, A.; Castillo, R. J. Comput. Aid. Mol. Des., 2004, [123] 18, 345-360.
- [124] Hopfinger, A.J.; Wang, S.; Tokarski, J.S.; Jin, B.Q; Albuquerque, M.; Madhav, P.J.; Duraiswami, C. J. Am. Chem. Soc., 1997, 119, 10509-10524.
- Bak, A.; Polanski, J. Bioorg. Med. Chem., 2006, 14, 273-279.
- [126] Ortiz, A.R.; Pisabarro, M.T.; Gago, F.; Wade, R.C. J. Med. Chem., 1995, 38, 2681-2691.
- [127] Rodríguez-Barrios, F.; Gago, F. J. Am. Chem. Soc., 2004, 126, 2718-